HHS Public Access

Author manuscript

Cancer Immunol Res. Author manuscript; available in PMC 2024 January 05.

Published in final edited form as:

Cancer Immunol Res. 2023 July 05; 11(7): 925–945. doi:10.1158/2326-6066.CIR-22-0444.

Feasibility and Safety of Personalized, Multi-Target, Adoptive Cell Therapy (IMA101): First-In-Human Clinical Trial in Patients with Advanced Metastatic Cancer

Apostolia M Tsimberidou[1], **Kerstin Guenther**[2], **Borje S Andersson**[3], **Regina Mendrzyk**[2], **Amir Alpert**[4], **Claudia Wagner**[2], **Anna Nowak**[2], **Katrin Aslan**[2], **Arun Satelli**[4], **Fabian Richter**[2], **Sabrina Kuttruff-Coqui**[2], **Oliver Schoor**[2], **Jens Fritsche**[2], **Zoe Coughlin**[4], **Ali S Mohamed**[4], **Kerry Sieger**[4], **Becky Norris**[1], **Rita Ort**[1], **Jennifer Beck**[1], **Henry Hiep Vo**[1], **Franziska Hoffgaard**[2], **Manuel Ruh**[2], **Linus Backert**[2], **Ignacio I Wistuba**[5], **David Fuhrmann**[2], **Nuhad K Ibrahim**[6], **Van Karlyle Morris**[7], **Bryan K Kee**[7], **Daniel M Halperin**[7], **Graciela M Nogueras-Gonzalez**[8], **Partow Kebriaei**[3], **Elizabeth J Shpall**[3], **David Vining**[9], **Patrick Hwu**[10,†], **Harpreet Singh**[11], **Carsten Reinhardt**[11], **Cedrik M Britten**[11], **Norbert Hilf**[2], **Toni Weinschenk**[11], **Dominik Maurer**[2], **Steffen Walter**[4]

[1]Department of Investigational Cancer Therapeutics, The University of Texas MD Anderson Cancer Center, 1515 Holcombe Blvd., Houston, Texas 77030, USA

[2]Immatics Biotechnologies GmbH, Paul-Ehrlich-Str. 15-17, 72076 Tuebingen, Germany

Corresponding author: Apostolia-Maria Tsimberidou, M.D., Ph.D., Professor, The University of Texas MD Anderson Cancer Center, Department of Investigational Cancer Therapeutics, Unit 455, 1515 Holcombe Boulevard, Houston, TX 77030, Phone: 713-792-4259, Fax: 713-794-3249, atsimber@mdanderson.org.

[†]Current address: Moffitt Cancer Center, 12902 USF Magnolia Dr, Tampa, Florida 33612, USA

All remaining authors have declared no conflicts of interest.

Authors' Disclosures

Apostolia M. Tsimberidou: Clinical Trial Research Funding (Institution): IMMATICS, Parker Institute for Cancer Immunotherapy, Tempus, OBI Pharma, EMD Serono, Baxalta, ONYX, Bayer, Boston Biomedical, Placon Therapeutics, Karus Therapeutics, Tvardi, Novocure, CPRIT; Travel, Accommodations, Expenses: ASCO, Genentech, Covance, Tempus; Consulting or Advisory Role: VinceRx, Diaccurate, BrYet, Nex-I, and Macrogenics.

Ignacio I. Wistuba: Advisory Board (honoraria): Genentech/Roche, Bayer, Bristol-Myers Squibb, Astra Zeneca, Pfizer, HTG Molecular, Asuragen, Merck, GlaxoSmithKline, Guardant Health, Flame, Novartis, Sanofi, Daiichi Sankyo, Amgen, Oncocyte, and MSD; Speaker (honoraria): Medscape, Genentech/Roche, Platform Health, Pfizer, AstraZeneca, Merck; Research support (to the institution): Genentech, HTG Molecular, DepArray, Merck, Bristol-Myers Squibb, Medimmune, Adaptive, Adaptimmune, EMD Serono, Pfizer, Takeda, Amgen, Karus, Johnson & Johnson, Bayer, Iovance, 4D, Novartis, and Akoya.

Van Karlyle Morris: Research Funding: Boehringer Ingelheim and Immatics. Research Funding (Institution): Bristol-Myers Squibb, Array Biopharma, and EMD Serono. Honoraria: Products in Knowledge. Consulting or Advisory Role: Array Biopharma, Incyte, SERVIER, Boehringer Ingelheim.

Daniel M. Halperin: Research Support: Novartis, ITM, Tarveda, Genentech; Consulting/Advising: Novartis, ITM, Chimeric Therapeutics, Chiasma/Amryt, TerSera, Ipsen, Crinetics; DSMB: Alphamedix.

Elizabeth J. Shpall: Consultant on Scientific Advisory Boards: Novartis, Magenta, Adaptimmune, Axio, Navan; License Agreements or Patents: Takeda, Affimed; Honorarium: Magenta, Novartis, Bayer HealthCare Pharmaceuticals.

David Vining is the CEO and majority owner of VisionSR and an inventor of Bracco Diagnostics.

Patrick Hwu: Scientific Advisory Board Member: Immatics, Dragonfly

Harpreet Singh is CEO of Immatics N.V.

Cedrik M. Britten, Carsten Reinhardt and **Toni Weinschenk** are managing directors of Immatics N.V.

Kerstin Guenther, Regina Mendrzyk, Claudia Wagner, Anna Nowak, Katrin Aslan, Fabian Richter, Sabrina Kuttruff-Coqui, Oliver Schoor, Jens Fritsche, Franziska Hoffgaard, Manuel Ruh, Linus Backert, David Fuhrmann, Norbert Hilf and Dominik Maurer are employees of Immatics Biotechnologies GmbH.

Amir Alpert, Arun Satelli, Zoe Coughlin, Ali Mohamed, Kerry Sieger and Steffen Walter are employees of Immatics US Inc.

[3]Department of Stem Cell Transplantation and Cellular Therapy, The University of Texas MD Anderson Cancer Center, 1515 Holcombe Blvd., Houston, Texas 77030, USA

[4]Immatics US, Inc., 2201 Holcombe Blvd., Suite 205, Houston, Texas 77030, USA

[5]Department of Translational Molecular Pathology, The University of Texas MD Anderson Cancer Center, 1515 Holcombe Blvd., Houston, Texas 77030, USA

[6]Department of Breast Medical Oncology, The University of Texas MD Anderson Cancer Center, 1515 Holcombe Blvd., Houston, Texas 77030, USA

[7]Department of Gastrointestinal Medical Oncology, The University of Texas MD Anderson Cancer Center, 1515 Holcombe Blvd., Houston, Texas 77030, USA

[8]Department of Biostatistics, The University of Texas MD Anderson Cancer Center, 1515 Holcombe Blvd., Houston, Texas 77030, USA

[9]Department of Abdominal Imaging, The University of Texas MD Anderson Cancer Center, 1515 Holcombe Blvd., Houston, Texas 77030, USA

[10]Department of Melanoma Medical Oncology, The University of Texas MD Anderson Cancer Center, 1515 Holcombe Blvd., Houston, Texas 77030, USA

[11]Immatics N.V., Paul-Ehrlich-Str. 15-17, 72076 Tuebingen, Germany

Abstract

IMA101 is an actively personalized, multi-targeted adoptive cell therapy (ACT), whereby autologous T cells are directed against multiple novel defined peptide-HLA (pHLA) cancer targets. HLA-A*02:01-positive patients with relapsed/refractory solid tumors expressing ≥1 of 8 pre-defined targets underwent leukapheresis. Endogenous T cells specific for up to 4 targets were primed and expanded *in vitro*. Patients received lymphodepletion (fludarabine, cyclophosphamide), followed by T-cell infusion and low-dose interleukin-2 (Cohort 1). Patients in Cohort 2 received atezolizumab for up to 1 year (NCT02876510). Overall, 214 patients were screened, 15 received lymphodepletion (13 women, 2 men; median age, 44 years), and 14 were treated with T-cell products. IMA101 treatment was feasible and well tolerated. The most common adverse events were cytokine release syndrome (Grade 1, n=6; Grade 2, n=4) and expected cytopenias. No patient died during the first 100 days after T-cell therapy. No neurotoxicity was observed. No objective responses were noted. Prolonged disease stabilization was noted in three patients lasting for 13.7, 12.9, and 7.3 months. High frequencies of target-specific T cells (up to 78.7% of $CD8^+$ cells) were detected in the blood of treated patients, persisted for >1 year, and were detectable in post-treatment tumor tissue. Individual TCRs contained in T-cell products exhibited broad variation in TCR avidity, with the majority being of low-avidity. High-avidity TCRs were identified in some patients' products. This study demonstrates the feasibility and tolerability of an actively personalized ACT directed to multiple defined pHLA cancer targets. Results warrant further evaluation of multi-target ACT approaches using potent high-avidity TCRs.

Keywords

adoptive cell therapy; immunotherapy; advanced cancer; clinical trial; phase 1; personalized medicine; IMA101; multi-target

INTRODUCTION

Adoptive cell therapy (ACT) using endogenous antigen-specific T lymphocytes against tumors is a promising personalized cancer immunotherapy approach, as T-cell products from the endogenous T-cell repertoire are expected to lack fatally self-reactive T cells. Encouraging clinical outcomes and a favorable toxicity profile have been described for endogenous ACT in patients with melanoma and leukemia (1–4). In 2016, when the study was conceptualized, antigen-specific ACT was limited to targeting a few previously described antigens, such as CD19 in hematological malignancies and MART-1, MAGE, gp100, WT1, or NY-ESO-1 in solid tumors (5,6). One study with autologous, non-engineered T cells targeting NY-ESO-1 demonstrated the feasibility of treating metastatic melanoma with NY-ESO-1–specific $CD4^+$ T cells generated from the blood of an unimmunized patient (2). A phase I/II study of autologous anti-MAGEA3 T-cell receptor (TCR)-engineered T cells demonstrated clinical regression of the tumors in five (55.6%) of nine patients with metastatic cancer (7). In another study, autologous TCR-transduced T cells for NY-ESO-1-positive tumors induced objective responses in 4 of 6 patients with synovial cell sarcoma and 5 of 11 patients with melanoma. Complete regression persisted after 1 year in 2 of 11 patients with melanoma; 1 patient with synovial cell sarcoma had a partial response lasting 18 months (8). In a long-term follow-up study, objective responses were observed in 11 of 18 patients with sarcoma and 11 of 20 patients with melanoma (9). In another study of autologous TCR-engineered T cells recognizing a naturally processed peptide shared by the cancer-testis antigens NY-ESO-1 and LAGE-1, clinical responses were observed in 16 of 20 patients with advanced cancer, and the median progression-free survival (PFS) was 19.1 months (10). In addition to these promising results, relevant adverse effects caused by the expression of some targeted antigens in normal tissues have been reported (5,11). Additionally, tumors may escape treatment when the only tumor antigen targeted is lost (12) or when the distribution of the tumor antigen is heterogeneous due to clonal evolution (13).

Overall, these reports indicate that additional targets may be needed for ACT, particularly for solid tumors, and that more clinical research including autologous endogenous T-cell therapy is warranted. IMA101 is an actively personalized, multi-targeted ACT that aims to avoid these shortcomings by using autologous T-cell products against multiple defined tumor-associated, peptide-human leukocyte antigen (pHLA) targets in combination with an optimized lymphodepleting chemotherapy regimen, low-dose interleukin (IL)-2, and a checkpoint inhibitor. Target antigen peptides in the tumor target warehouse were derived from PRAME, MAGEA1, MAGEA4, MAGEA8, NY-ESO-1, COL6A3 exon 6, MXRA5, and MMP1, which have no or very limited expression in normal tissues (14) (Supplemental Table S1). Naturally occurring, antigen-specific T cells are primed, expanded, and sorted *in vitro* with IL21, generating T cells with a less terminally differentiated phenotype (4,15).

In addition to the selection of novel target antigens to generate specific T-cells, we used an optimized lymphodepletion regimen and low-dose IL2 (1.0×10^6 IU, s.c. twice daily) to enhance T-cell survival and expansion (16,17). Lymphodepleting regimens, mostly fludarabine (FLU) and cyclophosphamide (CY) combinations, have been described to facilitate T-cell engraftment and persistence (6,18,19). To further enhance responses to endogenous T-cell therapy, checkpoint inhibitors have been used and have achieved durable clinical responses that correlate with *in vivo* persistence, recovery of a central memory phenotype of transferred T cells, and induction of antigen spreading (20). Blockade of the PD-1/PD-L1 interaction by checkpoint inhibitors combined with tumor-specific T cells may reduce the intratumoral inhibition of the transferred T cells, resulting in synergism and improving the clinical outcomes achieved with either modality alone (21,22). Early studies demonstrate improved response rates and T-cell persistence (23–25).

Based on the considerations outlined above, we conducted a first-in-human study of IMA101 in human leukocyte antigen (HLA)-A*02:01-positive patients with advanced, metastatic cancer expressing ≥1 of the aforementioned pHLA cancer targets. Patients received lymphodepletion, followed by infusion of 1–4 T-cell products and low-dose IL2. IMA101 was investigated as a monotherapy (Cohort 1) or in combination with atezolizumab (anti-PD-L1; Cohort 2). The primary objective was to assess safety and tolerability; secondary objectives were to evaluate the *in vivo* persistence of transferred T cells and to assess tumor response. Assessment of PFS, overall survival (OS), feasibility, and biomarkers were exploratory objectives.

PATIENTS AND METHODS

Patients and eligibility criteria

The protocol was approved by the Food and Drug Administration and the Institutional Review Board at The University of Texas MD Anderson Cancer Center. The study was conducted in accordance with the Declaration of Helsinki and the International Conference on Harmonization Good Clinical Practice guidelines. All the study participants provided written informed consent before enrollment on the individual clinical trials in which they participated. The study was registered in www.clinicaltrials.gov (NCT02876510) and approved by the Western Institutional Review Board (WIRB, tracking number 20162235). All patients signed the informed consent form stating that they were aware of and agreed with the investigational nature of the study.

Screening and leukapheresis eligibility criteria included patients who were ≥18 and ≤65 years of age (to select for patients with sufficient proliferative capacity of T cells), had pathologically confirmed advanced/metastatic cancer prior to enrollment, and tested positive for human leukocyte antigen phenotype HLA-A*02:01 (4-digit high-resolution of HLA phenotype performed by a Clinical Laboratory Improvement Amendments-certified laboratory was acceptable). Other eligibility criteria included an Eastern Cooperative Oncology Group (ECOG) performance status of 0 or 1; life expectancy >6 months prior to enrollment; adequate organ and marrow function (absolute neutrophil count ≥1,000/μL and platelets ≥100,000/μL, unless these abnormalities were due to bone marrow involvement; Hb ≥8 g/dL); ≥1 accessible lesion (metastasis or primary tumor) by non-high-risk collection

procedures for biopsy; and availability of a further line of therapy (prior to treatment with IMA101). Adequate hepatic function (total bilirubin level ≤2 x the upper limit of normal [ULN], unless the patient has known Gilbert's syndrome; alanine aminotransferase [ALT] and aspartate aminotransferase [AST] levels ≤ 3 x ULN or ≤ 5 x ULN for patients with liver metastases); adequate pulmonary function (FEV1, FVC, and DLCO1 ≥ 50% predicted [corrected for Hb]; oxygen saturation > 92% on room air); acceptable coagulation status (international normalized ratio [INR] of prothrombin time [PT] of blood coagulation ≤ 2.0 x ULN and partial thromboplastin time [PTT] ≤ 2.0 x ULN); and estimated serum creatinine clearance ≥ 50 mL/min by the Cockcroft-Gault formula were also required.

Female patients of childbearing potential had to agree to use adequate contraception (hormonal or barrier method of birth control; abstinence) prior to study entry and for the duration of study participation. Male patients had to agree to use effective contraception or abstinence while on study and for 90 days after infusion of the IMA101 T-cell product. Women were considered to be of childbearing potential if they had had menses within the past 12 months and had not had a tubal ligation, hysterectomy, or bilateral oophorectomy. A female patient had to inform her treating physician immediately if she knew or suspected that she was pregnant while participating in this study.

Patients signed an informed consent document at the time of biomarker screening and leukapheresis and at the time of screening for treatment, stating that they were aware of the investigational nature of the study. Other criteria included confirmed availability of production capacities for the patient's IMA101 products. Patient tumors had to express ≥1 tumor target, as assessed by quantitative PCR (qPCR) analysis of a tumor biopsy. For all selected study targets, a correlation between mRNA and immunopeptidome levels was established, as previously described (26). Targets were considered positive if levels were above a target specific delta-Ct threshold that was chosen to maximize the sensitivity and specificity of prediction of peptide presentation (MAGEA4: 8.73, NY-ESO-1: 12.09, PRAME: 4.75, COL6A3: 4.94, MXRA5: 2.08, MAGEA1: 7.83, MAGEA8: 7.58, MAGEA4: 7.26, MMP1: 6.30) (26). Patients previously screened but not eligible for other Immatics trials based on tumor biomarker testing with the same qPCR assay whose tumors were positive for at least 1 tumor antigen could enter screening in order to avoid a new tumor biopsy and repeated biomarker testing.

Patients were excluded from screening and leukapheresis if they had any condition contraindicating leukapheresis collection, human immunodeficiency virus (HIV) infection, active hepatitis B or C infection, or active infections requiring oral or IV antibiotics or that could cause a severe disease and pose a severe danger to lab personnel working on the patient's blood or tissue. If test results were not indicative of an active infection, patients could be included. Patients who had a history of other malignancies (except for adequately treated basal or squamous cell carcinoma or carcinoma *in situ*) within the last 3 years and/or brain metastases were excluded unless an imaging scan with contrast enhancement not older than 4 weeks demonstrated no evidence of currently active brain metastasis and their disease was stable. Patients were also excluded if they had received systemic corticosteroids for a chronic condition within 2 weeks prior to leukapheresis or had received other therapies, including chemotherapy, surgery, radiotherapy, tyrosine kinase inhibitor, and investigational

drugs, less than approximately 7 days prior to leukapheresis. Other exclusion criteria included extensive radiotherapy to the lung or liver within 4 months prior to the start of the lymphodepletion regimen and cardiac conditions which included uncontrolled hypertension (blood pressure > 150/100 mmHg) despite optimal therapy, uncontrolled angina, ventricular arrhythmias, congestive heart failure (New York Heart Association Class II or above), baseline left ventricle ejection fraction (LVEF) ≤ 50%, prior or current cardiomyopathy, atrial fibrillation with heart rate > 100 bpm, and unstable ischemic heart disease (myocardial infarction within 6 months prior to starting treatment or angina requiring use of nitrates more than once weekly). Additional exclusion criteria included prior stem cell transplantation or solid organ transplantation; concurrent severe and/or uncontrolled medical disease that could compromise participation in the study (i.e., uncontrolled diabetes, severe infection requiring active treatment, severe malnutrition, chronic severe liver or renal disease); and active diverticulitis, intra-abdominal abscess, gastrointestinal obstruction, abdominal carcinomatosis, or other known risk factors for bowel perforation. Other exclusion criteria included pregnancy or breastfeeding; serious autoimmune disease (at the discretion of the treating attending); history of active serious inflammatory bowel disease (including Crohn's disease and ulcerative colitis); autoimmune disorders such as rheumatoid arthritis, systemic progressive sclerosis (scleroderma), systemic lupus erythematosus, or autoimmune vasculitis (e.g., Wegener's granulomatosis); and history of hypersensitivity to CY, FLU, or IL2. Patients were excluded if they had immunosuppression not related to prior treatment for malignancy, history of or current immunodeficiency disease or prior treatment compromising immune function (at the discretion of the treating physician), or any other condition that would, in the investigator's judgment, contraindicate the patient's participation in the clinical study because of safety concerns or compliance with clinical study procedures.

To be eligible for treatment, patients had to have an ECOG performance status of 0 or 1; adequate hepatic function (total bilirubin ≤ 2 x ULN, unless the patient has known Gilbert's syndrome; ALT and AST levels ≤ 3 x ULN or ≤ 5 x ULN for patients with liver metastases); estimated serum creatinine clearance ≥ 50 mL/min (Cockcroft-Gault formula); and measurable disease. Patients were excluded from treatment if they had received chemotherapy, immunotherapy, surgery, or radiotherapy within the past 2 weeks or they had not recovered from Grade ≥ 2 adverse events of the previous therapy (except alopecia); had Grade 3–4 immune-related toxicities; had received extensive radiotherapy to the lung or liver during the 4 months prior to the start of the lymphodepletion regimen; were pregnant or breastfeeding; or had any other condition that would, in the investigator's judgment, contraindicate the patient's participation in the clinical study. Patients who would not be able to tolerate lymphodepletion, low-dose IL2, and/or IMA101 treatment, in the judgment of the investigator, were also excluded.

Prophylaxis

Acetaminophen (single 650 mg dose, orally) and diphenhydramine (single 50 mg dose, orally) were administered as prophylaxis against potential allergic reactions, and patients were closely monitored after the infusion of T cells. Prophylaxis against bacterial, viral, and fungal infections and neutropenic fever/sepsis was started on Day -6 of the lymphodepleting

regimen. Mesna (170mg/m^2 × 12 doses) was also administered as renal prophylaxis with CY (described below), according to institutional guidelines. Supportive care was delivered as per extant clinical routines. Growth factor support with colony stimulating factors (e.g., filgrastim [300 μg or 480 μg, weight dependent) was administered starting not earlier than Day 5 after T-cell infusion, unless clinically indicated. All FDA-approved medications administered on this protocol were provided by MD Anderson Pharmacy (vendor, Cardinal Health).

Patient monitoring

All patients were screened and treated at The University of Texas MD Anderson Cancer Center. Patients were admitted to the inpatient service of the Department of Stem Cell Transplantation and were in the hospital for up to 21 days (for lymphodepletion, IMA101 treatment, and IL2 administration) starting on Day -7. During hospitalization, patients had daily laboratory tests that included complete blood count with differential, comprehensive metabolic panel, urinalysis, and measurement of magnesium, uric acid, C-reactive protein, lactate dehydrogenase (LDH), and ferritin levels.

Cytokine measurements to monitor CRS

Peripheral blood for serum cytokine measurements (IL6, IFNγ) was collected on Days -3, 0, 1, 3, 7, and 14 to monitor for cytokine release syndrome (CRS) (27,28). For serum cytokine analysis, ProcartaPlex Hu Cytokine / Chemokine Panel 1A 34 Plex Immunoassay Kit (CAT # EPX340–12167-901, ThermoFisher Scientific) was used in a Luminex 200 (Luminex Corp). Once blood was drawn in accordance with institutional procedures, the samples were placed in upright position for 20–30 minutes at 20–25°C. Samples were then centrifuged for 15 minutes at >1200xg at ambient temperature. Equal parts of supernatant serum were pipetted into cryovials and stored in −80°C until further testing. The assay protocol required the kit standards to be tested in duplicate and the undiluted serum samples in triplicates with 25μL volume in each well. Controls were not used in the assay. There were 7 standards for each analyte in the assay. Four-fold serial dilution was performed to the reconstituted standard six times to reach Standard 7. The standard curve values required 5 parameter logarithmic (5 PL) curve fit and was dependent on the 34 Plex Immunoassay Kit Lot Number (as provided by manufacturer). The concentration of samples were calculated by plotting the expected concentration of the standards against the net median fluorescent intensity generated by each standard.

Cell preparations

Peripheral blood mononuclear cells (PBMCs) were isolated from patient leukapheresis products and cryopreserved. A list of raw materials and reagents used in IMA101 manufacturing is provided in Supplemental Table S2.

Preparation of PBMCs from leukapheresis samples

Cells were first removed from the leukapheresis sample bag and separated using a ficoll density gradient (Sepax). The PBMCs were then split into two equal portions. The first portion was directly cryopreserved in CryoStor 10 freezing media to be used in the

generation of monocyte-derived dendritic cells (DCs), whereas the second portion was CD25-depleted (CliniMACS) and cryopreserved in CryoStor CS10 to be used in the generation and enrichment of target specific T lymphocytes. Cells for each fraction were cryopreserved at 300×10^6 cells/vial.

Generation of dendritic cells (DCs)

Frozen patient PBMCs were thawed, washed, and plated at 10×10^6 to 15×10^6 cells per well (DCs were to result from ≈5% of the plated cells, and 1.8×10^6 DCs were needed per peptide stimulation) into 6-well plates. After 4 hours incubation, non-adherent cells were aspirated and the adherent cells (which were to mature into DCs) were incubated in AIM V media containing IL4 and GM-CSF. Every other day (on Days 2 and 4), AIM V media containing IL4 and GM-CSF was added into the wells containing maturing DCs. On Day 6, a maturation cocktail of AIM V media containing TNFα, IL1β, IL6, PGE-2, IL4, and GM-CSF was added to the cells. Finally, 20 to 48 hours after addition of the maturation cocktail, the DCs were harvested and either cryopreserved or moved directly into primary peptide stimulation.

Primary/secondary peptide stimulation

Overall, 1.8×10^6 DCs were removed per peptide antigen, and the appropriate peptide was added to a concentration of 40 μg/mL. β-2 microglobulin was added at 3 μg/mL if the peptide was Class I-restricted. The cell/peptide mixture was incubated at room temperature (RT) for four hours. During this four-hour period, the DC/peptide mixture was also irradiated with 5,000 rad (GammaCell 1000 Elite Cs-Best Theratronics, Ltd. Or Mark-I Model 68 Cs-JL Sheperd & Associates). Meanwhile, with no more than one hour of incubation time left, frozen CD25-depleted PBMCs were thawed, washed, and resuspended in CTL media with 10% human AB serum (CTL media was RPMI 1640 (Gibco catalog # A10491–01) supplemented with 10% heat inactivated human AB serum and 2% Glutamax). Overall, 70×10^6 autologous CD25-depleted PBMCs per peptide were removed and suspended in 50 mL CTL media with 10% serum with IL21 added. PBMCs were plated into a 48-well plate for each peptide. The irradiated DC/peptide mixture was washed in PBS/ethylenediaminetetraacetic acid (EDTA) + 1% HSA and resuspended in CTL media with 10% serum. The cells were added into the 48-well plate containing the PBMCs, mixed well, and incubated, at 37°C. On Day 2 to 4, fresh CTL media with 10% human AB serum and IL21 was added into the wells. Seven days after stimulating the cells with peptide, the cells were entered into the secondary peptide stimulation procedure.

The procedure to peptide pulse the DCs for the secondary stimulation was the same as for primary stimulation. During the four-hour incubation of the DC/peptide mixture, the primary stimulation plates were removed from the incubator. Approximately 70% of the media was aspirated from each well, while the cells settled at the bottom of each well were not disturbed. Each well was brought up to 900 μL using CTL media with 10% human AB serum. The cells and media in each well were mixed well. The plates were returned to the incubator at 37°C until the DCs had completed their four-hour incubation with peptide. At the end of the four-hour incubation and irradiation, the DCs were washed with PBS/EDTA + 1% HSA and resuspended in CTL media with 10% serum and IL21. The CTL media/DC

mixture was added into each well of the peptide plate containing primary stimulated cells. The plates were incubated at 37°C overnight. The next day, a mixture of CTL media with 10% human AB serum, IL2 and IL7 was added to each well. On Day 3, 70% of the media was aspirated from each well (without disturbing the cells at the bottom of the well) and the volume was brought back up to 1 mL with CTL media with 10% human AB serum containing IL21. The cells were returned to the incubator at 37°C. Five to eight days after stimulation, 150 μL were removed from each well and analyzed by flow cytometry for live/dead, CD8, and tetramer. The positive wells were pooled and underwent the cell sorting procedure.

Tetramer staining and cell sorting

Peptide-HLA tetramers that bind to the cognate TCR were used to isolate antigen-specific T cells. The pHLA monomer was biotinylated and multimerized to avidin conjugated to the fluorochrome PE to yield MHC-peptide tetramers. Positive and negative wells from each 48-well plate were selected based on their tetramer positivity, and combined in separate tubes. Each of the tubes containing the cells from the selected wells were washed, and resuspended in the running buffer comprised of PBS, 1% HSA, and 90 U/mL benzonase nuclease. The supernatant from the tetramer positive pooled wells was submitted for aerobic/anaerobic sterility testing. The tetramer positive cells were then stained with the specific tetramer at a concentration of 3 μg/mL and incubated at room temperature in the dark for 15 minutes. Following incubation, the cells were washed and resuspended in the running buffer. The cells were filtered through a 20 μm filter into a 10 mL syringe and injected into separate closed system, single use, sorting Tyto Cartridges. The tetramer positive cartridge was loaded into the Miltenyi MACSQuant Tyto®, and the sort was performed while keeping the cells at 4˚C. Upon completion of the sort, the sorted tetramer positive cells were removed from the cartridge and dispensed directly into the prepared rapid expansion protocol vessel containing feeder cells. The used cartridge was then discarded.

Rapid expansion protocol 1

The rapid expansion protocol (REP) 1 procedure required use of a frozen irradiated lymphoblastic cell line (LCL) culture as allogenic feeder cells. Prior to REP initiation, it was ascertained that there were 5×10^6 irradiated LCLs available for the initiation of a G-Rex 10 of sorted antigen-specific T cells. For each G-Rex 10, 5×10^6 frozen irradiated LCLs were thawed, washed, and resuspended in CTL media with 10% human AB serum, then incubated at 37°C until used as feeder cells. Normal donor (ND) PBMCs, also used as allogenic feeder cells, were prepared. For each G-Rex, 25×10^6 frozen irradiated ND PBMCs were thawed, resuspended in CTL media with 10% human AB serum, then incubated at 37°C until used as feeder cells. The ND PBMCs were irradiated with 5,000 rad and the LCLs were irradiated with 8,000 rad. The two cell types were pooled and suspended in CTL media with 10% human AB serum with 30 ng/mL CD3 Pure (OKT-3) added. The cells were then aliquoted into a G-Rex 10, and all available sorted antigen-specific T cells (obtained from previous section) were added to the G-Rex 10. The G-Rex were incubated overnight at 37°C. The next day, IL2 was added to 50 IU/mL. The G-Rex were returned to the incubator. On Day 4, ≈80% of the spent media was removed from the G-Rex 10, and fresh CTL media with 10% human AB serum and IL2 was added. On Day 6 and 7, IL2 was added to each G-Rex 10 to

50 IU/mL. On Day 8 and 9, a cell count was performed for each G-Rex 10. If the total viable cell number was $< 2 \times 10^8$, IL2 was added to 50 IU/mL and returned to the incubator. If the viable cell number was $\geq 2 \times 10^8$, the cells were transferred to a G-Rex 100 and brought up to 200 mL with fresh CTL media with 10% human AB serum and IL2 at 50 IU/mL. On Day 10 to 12, IL2 was added to each G-Rex to 50 IU/mL. On Day 13 and 14, cells were moved directly into REP 2.

Rapid expansion protocol 2 (REP 2)

The REP 2 was a two-week culture that resulted in greater than 100-fold expansion of a patient's antigen-specific T cells. The dose per patient was a maximum of 4×10^{10} total T cells with a maximum of 1.75×10^{10} T cells from each antigen-specific drug product. Up to nine G-Rex 100 M were initiated per drug substance. Prior to REP initiation, it was ascertained that there were sufficient LCLs cryopreserved for the number of G-Rex 100M to be initiated in the REP (2×10^8 cells/G-Rex 100M). LCLs were thawed, washed, and resuspended in CTL media with 10% human AB serum, then incubated at 37°C until used as feeder cells. Prior to REP initiation, it was ascertained that there were sufficient ND PBMCs cryopreserved for the number of G-Rex 100M to be initiated in the REP (1×10^9 cells/G-Rex 100M). ND PBMCs were thawed, washed, and resuspended in CTL media with 10% human AB serum, then incubated at 37°C until used as feeder cells. Appropriate numbers of irradiated LCLs and ND PBMCs were combined in each G-Rex 100M, and the volume was brought up to 400 mL with CTL media with 10% human AB serum and 30 ng/mL CD3 Pure (OKT-3). G-Rex were incubated at 37°C until use. One to 5×10^6 antigen-specific T cells were transferred into each G-Rex 100M with the irradiated LCLs and ND PBMCs, and the G-Rex were placed in the 37°C incubator overnight. The next day, IL2 was added to 50 IU/mL. On Day 4, each G-Rex flask was filled to 800 mL with CTL media with 10% human AB serum and IL2 added to 50 IU/mL. On Day 6 and 7, IL2 was added to 50 IU/mL. On Day 8 and 9, 300 mL of spent media were exchanged and each G-Rex 100M was filled to 1000 mL with CTL media with 10% human AB serum and IL2 added to 50 IU/mL. On Day 10 and 11, cells were counted. If ≤ 5 G-Rex 100M were in culture for a particular drug substance, each G-Rex 100M was split into 2 G-Rex 100M if total viable cell count was $> 2 \times 10^9$ T cells (if $< 2 \times 10^9$ T cells, IL2 was added into media at 50 IU/mL.). Each G-Rex 100M was filled to 1000 mL with CTL media with 10% human AB serum and IL2 added to 50 IU/mL. If ≥ 6 G-Rex 100M were in culture for a particular drug substance, 25% of cells from each G-Rex 100M were pooled and cryopreserved if total viable cell count was $> 2 \times 10^9$ T cells (If $< 2 \times 10^9$ T cells, IL2 was added into media at 50 IU/mL). Each remaining G-Rex 100M was filled to 1000 mL with CTL media with 10% human AB serum and IL2 added to 50 IU/mL. Two to four days later, cells were harvested, counted, and cryopreserved using CryoStor CS10.

Tumor marker screening

A target discovery platform was used to identify and select the pHLA targets for the tumor target warehouse used in this trial and to define thresholds for patient inclusion (26). Tumor biopsy (core needle biopsy/fine-needle aspiration/excision) was performed in HLA-A*02:01-positive patients and tested for the expression of each of the warehouse targets using a qPCR assay. The biopsy cores on collection were immediately stored in RNAlater™

solution (CAT# AM7022, Thermo Fisher Scientific) to protect RNA integrity in the samples. Tissue was homogenized and RNA was extracted using All Prep DNA/RNA extraction kit (CAT#80204, Qiagen). For RNA quantification, RNA ScreenTape assay (CAT# 5067–5576, Agilent) was used in TapeStation 2200 (Agilent). Extracted RNA (0.02 to 2 μg) was reverse transcribed using High-Capacity Reverse Transcription kit (Cat#4368814, Applied Biosystems) in a ProFlex™ PCR System Thermal cycler (Applied biosystems). A minus reverse transcriptase (-RT) reaction was also performed along with cDNA synthesis reaction. An input of 10 ng/well was used for qPCR using TaqMan Fast advanced Master Mix (CAT# 4444965, Applied Biosystems). The qPCR assay was performed on pre-manufactured custom coated plates with dried-down inventoried TaqMan gene expression assays (Life Technologies, Thermo Fisher Scientific). The assay required cDNA templates to be run in triplicate wells, no template control in duplicate wells and -RT in single wells. The qPCR plates were run on a 7500 Real-Time PCR System (Applied Biosystems). Delta Ct (DCt) was determined by subtracting the average Ct value of the reference genes from the target gene Ct value and was compared to the pre-established target DCt threshold to determine target expression in the patient biopsy. Only patients with tumors that expressed ≥ 1 IMA101 target by qPCR were eligible to participate in the study. All targets expressed in a patient's tumor were ranked according to their pre-determined immunogenicity, and up to four targets were selected for production of personalized autologous IMA101 T-cell products. For immunogenicity testing of IMA101 warehouse peptides prior to the clinical trial, target-specific T cells from healthy donors were primed and expanded *in vitro*. In brief, $CD8^+$ T cells from the leukapheresis of a HLA-A*02+ healthy donor were primed and stimulated using two rounds of culture with autologous peptide-pulsed DCs in the presence of IL21, IL2, and IL7. Immunogenicity ranking was based on number of positive donors, *i.e.*, donors for which $CD8^+$ T cells could be primed for the respective peptide.

IMA101 manufacturing

The manufacture of IMA101 followed the method developed by Chapuis et al (4). Briefly, PBMCs were isolated from the patient leukapheresis products and stored as described. Target-specific T cells were stimulated and expanded in the presence of IL-21, utilizing CD25-depleted PBMCs and target peptide-pulsed autologous dendritic cells (DCs). Up to four T-cell specificities per patient were stimulated in separate cultures and expanded. Antigen-specific T cells were then enriched using HLA multimer-guided flow sorting (Miltenyi Tyto multimer generation and flow cytometry described below) resulting in a tetramer-positive T cell purity ranging from 71.4% to 100.0% and further expanded in the presence of irradiated allogenic feeder cells and cytokines before harvesting and cryopreservation. The duration of the T-cell product manufacturing was approximately 3–4 months, including the release testing requirements. The T-cell products were cryopreserved until administration to the patient was indicated (e.g., after disease progression on bridging therapy).

Allogeneic PBMC feeder cells

Pooled ND PBMCs used as allogeneic feeder cells in both REP 1 and REP 2 were obtained from non-mobilized normal donors by leukapheresis. The leukapheresis units were obtained from Carter BloodCare, Gulf Coast Regional Blood Center, or other FDA-licensed

vendors. Gulf Coast Regional Blood Center (Houston, TX) is a non-profit organization and is accredited, licensed and inspected by the FDA, American Association of Blood Banks (AABB), as well as local and state authorities. Carter BloodCare (Bedford, TX) is an AABB-accredited blood center, certified by the Foundation for the Accreditation of Cellular Therapy, and licensed by the FDA. These two vendors were used as the source of donor PBMC leukapheresis. Donors for these products have been screened and tested for infectious diseases before collection of their product and determined to be negative before being used as feeders. At minimum, these tests included screening for HBC, HBSAG, HCV, HIV-1/2, HTLV-I/II, IAT, NAT, STS, and WNV. Normal donors from Carter BloodCare and Gulf Coast Regional Blood Center were screened and tested per collection facility standard procedure using FDA-licensed, approved, or cleared screening tests. The donors were screened and evaluated per 21 CFR 1271 subpart C and communicable disease testing was performed by testing laboratories certified (21 CFR 1271.55(b)(1)) to perform such testing on human specimens under CLIA and 42 CFR 493, or equivalent requirements as determined by the Center for Medicare and Medicaid Services. In addition, prepared pooled donor PBMCs were tested for bacterial and fungal sterility, mycoplasma, and endotoxin. Leukapheresis units for PBMC feeder's preparation were received at the GMP facility within 24 hours after the completion of the leukapheresis procedure scheduled by the collection facility and were processed and cryopreserved by Immatics trained personnel at Immatics' dedicated GMP suites at the UTH GMP facility. Once cryopreserved, the feeder PBMCs were irradiated with 5,000 rad and stored in vapor phase of liquid nitrogen until released per Certificate of Analysis (CoA). Prior to use in the REP manufacturing process, irradiated ND feeder PBMC were thawed, washed, and resuspended in CTL media plus 10% human AB serum.

Allogeneic lymphoblastic cell line feeder cells

The TM-LCL was provided by City of Hope. This strain and its T-cell line have been extensively tested by City of Hope. The donor of the cells that were used to generate this LCL was screened for potential risk factors and tested for an infectious disease marker panel (except for West Nile which was not being tested at that time). Viral safety evaluation was performed in accordance with ICH Q5A (R1) Quality of Biotechnological Products: Viral Safety Evaluation of Biotechnology Products Derived from Cell Lines of Human or Animal Origin. This testing was in compliance with the requirements of 21 CFR Part 1271. The cells were tested and released on 20-Jul-2005. In addition to the testing listed on the CoA, the TM-LCL Cell Bank obtained from the City of Hope by Immatics has tested negative for both AAV and HPV at WuXi AppTec using validated GMP assays.

The TM-LCL Cell Bank from City of Hope was expanded by Immatics in Lonza X-VIVO 15 serum free media and maintained at a concentration of 1 to $10 \times 10^6/cm^2$ in G-Rex culture vessels. The expanded culture was cryopreserved as an Immatics working cell bank. Immatics working cell banks were tested for sterility, mycoplasma, endotoxin, and HLA matching. The TM-LCL was cultured in Lonza X-VIVO 15 serum-free media and maintained in culture for a period of time in order to generate active reagent cell banks. Each reagent cell bank was cryopreserved and irradiated with 8,000 rad and stored in vapor phase of liquid nitrogen until released per TM-LCL reagent cell bank specifications. Prior

to use in the REP manufacturing process, frozen irradiated LCLs were thawed, washed, and resuspended in CTL media plus 10% human AB serum.

Treatment and sample collection

Treatment consisted of lymphodepletion, IMA101 infusion, and IL2 (Figure 1). The lymphodepletion regimen was designed in 2016 and consisted of 40 mg/m² FLU (1-hour intravenous [IV] infusion, Fludara®, Genzyme Corporation), followed 1 hour later by 500 mg/m² CY (2-hour IV infusion, Baxter) on Days -6 to -3 (30,31). IMA101 products (up to 1.75×10^{10} cells per product, not exceeding 4×10^{10} cells in total) were thawed and infused intravenously (no wash) approximately 72 hours after completion of the lymphodepletion regimen (Day 0), allowing sufficient time for FLU clearance (32,33). IL2 treatment, 1.0×10^6 IU, administered every 12 hours s.c., was started within 6 hours after IMA101 (Days 0–14). Patients were treated with IMA101 monotherapy (Cohort 1) or with IMA101 and 1200 mg IV atezolizumab (Tecentriq, Genentech, F. Hoffman-La Roche) over 30–60 minutes, starting 3 weeks after IMA101 infusion and upon hematologic recovery and thereafter every 3 weeks for up to 1 year (Cohort 2), or until disease progression, unacceptable toxicity, patient withdrawal of consent or if the physician considered it in the interest of patient to discontinue. Patients received Mesna and other supportive care measures as per institutional guidelines. All patients underwent computed tomography or magnetic resonance imaging studies, including brain imaging, at baseline and approximately every 6 weeks after IMA101 treatment, unless otherwise clinically indicated, using state-of-the-art GE or Siemens scanners. Toxicity was assessed according to the National Cancer Institute Common Terminology Criteria of Adverse Events (CTCAE), version 5.0; cytokine release syndrome (CRS) (27,28) and immune effector cell-associated neurotoxicity syndrome (ICANS) were assessed using standard institutional CARTOX guidelines (34). Pre- (at the time of leukapheresis) and post-infusion on Day 1, 7, 14, 21, 56, 84, 126, 168, Month 9 and 12, and during follow up visits at Month 12 and 18, PBMCs for immunomonitoring were isolated within 8 hours of venipuncture from sodium heparin blood samples (BD Vacutainer® Heparin Tubes 10mL, BD, 367874) of patients by Ficoll–Hypaque density gradient centrifugation. Blood was diluted in DPBS (VWR, 392–0434) and 28 mL were carefully layered onto 15 mL Ficoll (PAN-Biotech, P04–60100) in Separation tubes (VWR, 720–1840). Samples were centrifuged for 15 minutes at 800xg without brakes and the upper content of the separation tubes was transferred to fresh tubes, washed with DPBS and centrifuged for 10 minutes at 320xg. The pellet was resuspended in 1% HSA (Octapharma, 5400949) in DPBS. Cell numbers of live PBMCs were determined in Neubauer counting chambers (Paul Marienfeld GmbH & Co. KG, 0640010) with Turk's solution (VWR, 93770) and 0.05% trypan blue (VWR, 1.11732.0025) in DPBS with 0.01% sodium azide (VWR, 8.22335.0100). Cells were cryopreserved at 10 to 20 Mio/ml in RPMI (Biozym, 880195) with 11.5% HSA and 10% DMSO (WAK Chemie, WAK-DMSO-70) until standardized assessment of immune responses. Apart from PBMC collection, tumor biopsy was collected to assess the presence of target biomarkers during screening. Additional biopsy was collected on Day 42 post-infusion. Optional biopsies were scheduled during the visit prior to treatment, and post treatment on Day 168, and Month 12 and 18 to assess T cell filtration into tumor. Tumor biopsy specimens were rinsed in RNALater™ to remove contaminating blood prior to processing.

Persistence, phenotype, and functionality of infused T cells

T-cell tracking by pHLA multimers by flow cytometry: For flow cytometry-based *ex vivo* immunomonitoring, isolated and cryopreserved PBMCs collected at different time points before and after infusion (specified above) were subjected to patient-individual pHLA-multimer and cell surface staining.

HLA-A*02:01-peptide monomers were produced by protein refolding from HLA-A*02:01 and β2 microglobulin *E.coli* inclusion bodies as previously described (41) with the following modifications. The HLA-A*02:01 heavy chain, with a biotinylation sequence for the BirA ligase at the C-terminus, and β2-microglobulin were expressed separately from a pET-3a vector in BL21(DE3)pLysS cells (Merck, 70236). Bacteria were cultured in LB medium supplemented with ampicillin (Roth, K029.1) and chloramphenicol (Merck, C0378) and induced with 1 mM isopropyl β-d-1-thiogalactopyranoside (VWR, 437144N) at an OD_{600} of 0.5 to 0.6. Cells were harvested 5 hours post-induction, resuspended in PBS (Gibco, 14190144) and frozen at −80°C. Magnesium chloride (10 mM, Merck, 105833), DNAse (10 μg/ml, Roche, 10104159001) and benzonase (50 U/ml, Merck, 1016950001) were added to the thawed cell suspension before sonication. Inclusion bodies were washed by repeated centrifugation and resuspension with 0.5% triton (Roth, 3051.2), 50 mM Tris, pH 8 (Roth, 4855.2), 100 mM NaCl (Roth, 3957.1), 1 mM EDTA (Roth, 8040.3), 0.1% sodium azide (Roth, K305.1) and 1 mM dithiothreitol (DTT, Roth, 6908.1). The pellet was finally dissolved in 8 M urea (Merck, U1250), 10 mM Tris pH 8, 100 mM di-sodium hydrogen phosphate dihydrate (Roth, 4984.2), 0.1 mM EDTA and 0.1 mM DTT.

For refolding, the heavy chain, β2-microglobulin and the peptide were added to the refolding buffer with a final concentration of 2.8 μM, 2.3 μM and 30 μM, respectively. The refolded monomer was purified by size exclusion chromatography (SEC) using the AEKTA go system (Cytiva) with a HiLoad 26/600 Superdex 75 pg column (Cytiva). Biotinylation with the BirA biotin-protein ligase (Avidity) was performed overnight at 27°C according to the manufacturer's instructions followed by a second purification by SEC. Biotinylated peptide-HLA monomers were multimerized using streptavidin conjugated to fluorochromes to yield tetramers (Streptavidin-PE, Life Technologies, S866; Streptavidin PE-Cy7, Biolegend, 405206). Multimers were incubated in PBS (Gibco, 14190–144), 2% fetal calf serum (FCS, Life Technologies, 10270–106), 2 mM EDTA (Roth, 8040.3), and 0.01% sodium azide (Roth, K305.1) with 25 nmol/ml biotin (Sigma-Aldrich, B4501) for 20 minutes at 4°C. Potential aggregates were removed by centrifugation for 60 minutes at 13000 rpm. PBMCs were rested overnight in RPMI 1640 (Life Technologies, A10491–01) + 10% human serum (C.C.Pro, S-41-M)+ 1 ng/mL IL15 (PromoCell, C-62512) and 20 U/mL IL2 (PZN 02238131). Between 5×10^5 and 5×10^6 cells were treated first with fixable Viability Stain BV510 (BD Biosciences, 564406) for 30 minutes at 4°C, followed by patient-individual multimer staining in phycoerythrin (PE) and/or PE-Cy7 for 20 minutes at room temperature (each multimer at a concentration of 1.25 μg/mL) and staining with surface markers using antibodies listed in Supplemental Table S3 for 30 minutes at 4°C in PBS, 2% FCS, 2 mM EDTA, and 0.01% sodium azide. All washing steps were carried out in PBS + 2% FCS + 2 mM EDTA + 0.01% sodium azide. Stained cells were fixed with PBS with 1% FCS and 1% formaldehyde (Sigma Aldrich, 47608) and acquired on a LSRII SORP

flow cytometer or a FACS AriaII and analyzed by FlowJo software, version 10.4 (Tree Star). Gating was performed using bi-dimensional dot plots with quadrants and/or polygon gates. The gating strategy was identical for all assay timepoints of a given patient. As a first step, irregularities were excluded using the time vs. PE gate. Next, doublets were excluded, and lymphocytes were gated for dump-channel negative and $CD3^+CD8^+$ T cells. Target-specific T cells were identified using the respective multimers. Phenotyping was performed within tetramer positive CD8 T cells (Supplemental Figure S6). As control, PBMCs from healthy donors were analyzed in every assay and stained with the same multimers as patient samples as well as irrelevant pHLAs.

***Ex vivo* class I intracellular cytokine staining assay:** Isolated and cryopreserved PBMCs collected at different time points before and after infusion were also used in an intracellular cytokine staining assay after stimulation with target peptides. Between 1.7 and 3.4×10^6 PBMCs per well were rested overnight, followed by incubation with antigenic peptide (10 μg/mL) in the presence of monensin (BD, 554724) and brefeldin A (BD, 555029) as per the manufacturer's instructions and CD107a BV605 (H4A3, BioLegend) (Supplemental Table S3) for 6 hours at 37 °C. Cells from each time point were stimulated with the corresponding target peptides. Cells stimulated with mock peptide (solvent only, DMSO (WAK Chemie, 0482) + 0.5% TFA (Merck, 108262)) were used as an internal negative control. After stimulation, PBMCs were treated with fixable Viability Stain BV510 (BD, 564406) for 20 minutes at 4°C, followed by surface staining as shown in Supplemental Table S3 for 20 minutes at 4°C in PBS + 2% FCS + 2 mM EDTA + 0.01% sodium azide. After a washing step in PBS + 2% FCS + 2 mM EDTA + 0.01% azide, cells were fixed using FACS Perm2 solution (BD, 558052) for 10 minutes at RT, and intracellular staining was carried out using PermWash (BD, 554723) and antibodies listed in Supplemental Table S3 for 30 minutes at 4°C.. Cells were acquired on a LSRII SORP flow cytometer and analyzed by FlowJo software, version 10.4.

The gating strategy was identical for all assay timepoints of a given patient. As a first step, irregularities were excluded using the time vs. PE gate. Next, doublets were excluded and lymphocytes were gated for dump-channel negative and $CD3^+$ T cells. Effector molecule expression (IFN-γ, TNF-α, IL-2, CD107a, MIP-1β) was analyzed within $CD8^+CD4^-$ T cells. Cytokine gates were set based on the populations in the mock control and the gating was applied to all samples of the patient (Supplemental Figure S8). In addition, these functional gates within $CD8^+CD4^-$ T cells, showing positivity or negativity for a given marker, were combined ("Boolean gates"). Out of 5 cytokines or markers, all $2^5 = 32$ possible combinatorial patterns were calculated using Boolean gating by FlowJo software, version 10.4. To be defined as an above-threshold response, the frequency of effector molecule-positive cells within one combinatorial pattern had to be at least two-fold over the frequency in the corresponding mock control.

TCRβ sequencing: Immunosequencing of the complementarity-determining region 3 (CDR3) of human TCRβ chains was performed with pHLA-multimer-sorted and unsorted T-cell products, peripheral blood, and serial tumor biopsy specimens collected prior to and 6 weeks after infusion using the immunoSEQ Assay (Adaptive Biotechnologies, Seattle,

WA) (35,36). Genomic DNA extracted from T-cell products, whole blood samples, or tumor biopsies was amplified in a bias-controlled multiplex PCR, followed by high-throughput sequencing. Genomic DNA was extracted from tumor biopsies using AllPrep DNA/RNA Mini kit (CAT# 80204, Qiagen) after tissue homogenization using Tissueruptor (Qiagen). Sequences were collapsed and filtered to identify and quantitate the absolute abundance of each unique TCRβ CDR3 region for further analysis, as previously described (35,36,42). To overcome PCR bias, a complete set of V-J templates were synthesized with unique barcodes. From this list of templates, PCR amplification was performed with a universal set of primers until each V-J template was amplified nearly equivalently, any residual bias was removed computationally. All TCRβ CDR3 regions were identified via alignment to genomic reference sequences from IMGT Database (www.imgt.org). The fractions of T cells in the samples were calculated by normalizing TCRβ template counts to the total amount of DNA usable for TCR sequencing, where the amount of usable DNA was determined by PCR amplification and sequencing of several housekeeping genes that were expected to be present in all nucleated cells. For each target-specific T-cell drug product, target-specific clones were identified as those comprising at least 1% of the drug product when sorted with antigen-specific multimers labelled with PE. Additionally, the maximum number of clones selected was capped at the number of wells that yielded successful *in vitro* priming during the T-cell manufacturing.

Cell lines

$CD8^+$ TCRαβ-knockout Jurkat cells (Promega, GA1162), acquired in 2020, were used for included data only in 2020, without authentication/re-authentication, and were handled according to manufacturers' recommendation, in culture for 2 to 4 weeks; mycoplasma testing was performed after 4 weeks of culture. T2 cells (Lymphoblast cell line, Human (Homo sapiens)), acquired from ATCC (CRL-1992) in 2010, without authentication/re-authentication, were handled according to manufacturers' recommendation, in culture for 2 to 4 weeks; mycoplasma testing was performed after 4 weeks of culture.

TCR identification and characterization

Sorting of target-specific T-cell clonotypes from patient T-cell products: The T-cell products from the first 5 patients treated were used for TCR identification (failed for ID01 for technical reasons). Additional T-cell products were randomly selected from further patients, with a focus on COL6A3 because COL6A3 was the target expressed most frequently. T-cell products were thawed, rested overnight, and stained via multiplexed 2D multimer staining (37,38) in addition to live/dead and anti-CD3 staining (Supplemental Table S3). Cells were sorted using a BD ARIAIII FACS device in 96-well plates containing lysis buffer (Tris 64.9 mM, LiCl 810.8 mM, EDTA 6.5 mM, pH 7.5) to be further processed by single-cell 5' Rapid Amplification of cDNA Ends (5' RACE). In-house-generated target HLA-monomers were multimerized to tetramers using commercially available, fluorochrome-labelled streptavidin reagents. COL6A3 and PRAME were labelled with APC (ThermoFisher, Lot 2009260)/PE (ThermoFisher, Lot 1973501) or APC (ThermoFisher, Lot 2009260)/BV711 (BD, Lot 8192727), NY-ESO-1 and MXRA5 with APC (ThermoFisher, Lot 2009260)/PE (ThermoFisher, Lot 1973501), and DDX5 (used as counterstain) with BV650 (Biolegend, Lot B267738)/PE-Cy7 (Biolegend, Lot B260327).

5’RACE and TCR coding sequence assembly: After lysis, mRNA was isolated using paramagnetic oligo(dT)-beads and cDNA synthesis was performed using TCR gene-specific primers. Subsequently, the TCR transcripts were amplified via nested multiplex PCR according to Kobayashi et al. 2013 (43) on a Veriti™ 96-Well Fast Thermal Cycler (Life technologies, Cat.# 4375305). Nucleotide sequences were obtained from Sanger sequencing, and the resulting data assembled into entire coding sequences *in silico* to determine germ line allele usage (BLAST algorithm) and CDR3 composition. Synthesized TCR genes were ordered via GenScript.

TCR re-expression: In order to generate a template for *in vitro* transcription (IVT), TCR alpha and beta chain DNA, including T7-Promoter (TAATACGACTCACTATAGGGAGA) (44) and Kozak sequences (GCCGCCACCATG) (45) at the 5’ end and a 64 adenosines 3’ tail adjacent to the stop codon, was synthesized by a commercial provider (Genscript biotech B.V., Nehterlands) and amplified by PCR. PCR was performed once per gene using PrimeSTAR® HS polymerase (TaKaRa bio Inc., Cat. #R040A) according to the manufacturers protocol, Primers T7Kozak (5’-AATAATACGACTCACTATAGGGAGAGCCGCCACC-3’) and pUC57_A64-B1 (5’-TTTTTTTTTTTTTTTTTTTTTTTTTTTTTTTTTTTTTTTTTTTTTTTTTTTTTTTTTTTTTT TTTTTTTTGACGGGCCCGGGATCCGAT-3’) on a Veriti™ 96-Well Fast Thermal Cycler (Life technologies, Cat.# 4375305). For re-expression, TCR mRNA was generated based on the PCR products by IVT using the mMESSAGE mMACHINE T7 Transcription Kit (Thermo Fisher Scientific, AM1344) according to the manufacturer’s protocol. TCRαβ-KO ($CD8^+$) Jurkat cells were harvested and electroporated with 20 μg mixed alpha and beta TCR mRNA using the ECM830 electroporator (BTX) at 500V, 3ms. The electroporated Jurkat cell samples were rested for 20 hours prior to starting co-culture assays as described below. Efficiency of TCR expression (30–70 % CD3-positive Jurkat cells) was assessed by flow cytometry after anti-CD3 and live/dead staining (Supplemental Table S3). TCR-mediated Jurkat activation is shown in the figures as RLU (relative luminescence units) values as acquired by the multiplate reader, after subtraction of background wells filled with medium only.

Determination of functional avidity: T2 cells were used as target cells and pulsed with the respective target peptides (MXRA5, NY-ESO, PRAME, COL6A3, PRAME as indicated in Figure 5 and Supplemental Figure S12) at concentrations ranging from 10 pM to 10 μM for 2 hours at 37°C. Subsequently, T2 cells and TCR-expressing TCRαβ-KO ($CD8^+$) Jurkat cells were washed with medium (RPMI 1640, Life technologies, 11875093 + 10% FCS, Gibco, A5256701+ 1% sodium pyruvate, CC Pro, Z-20-M + 1% MEM NEAA, Life technologies, 11140050 + 0.08% hygromycin B, Merck, 400052–50ML + 1% blasticidin, Fisher Scientific, 12172530) and seeded to a 96-well U bottom plate in a 1:1 ratio (5×10^4 T2 cells + 5×10^4 Jurkat cells). Following 6 hours of incubation at 37°C and 5% CO_2, the culture plates were analyzed using the Bio-Glo-NL Luciferase Assay System (Promega #J3082) according to the manufacturer’s protocol. Luciferase activity was determined as relative light units using a Synergy 2 microplate reader (BioTek) at a 0.5-second integration time. Data points were analyzed by GraphPad Prism (v8.4.0), and EC_{50} values calculated using a nonlinear regression model (4PL).

Multiplex immunofluorescence staining and image analysis

Multiplex immunofluorescence (mIF) analysis was performed in individual patients with evaluable pre- and post-treatment biopsy formalin-fixed, paraffin-embedded tissue as previously described (39,40) (Supplemental Table S3). Briefly, four-micrometer-thick, formalin-fixed, paraffin-embedded sample sections were stained using a mIF panel containing antibodies against cytokeratin (clone AE1/AE3, Dako), CD3 (cat#IS503, Dako), CD8 (clone C8/144B, Thermo Fisher Scientific), FOXP3 (clone D2W8E, Cell Signaling Technology), PD-1 (clone [EPR4877(2)], ABCAM), CD68 (clone [PG-M1 (M)], Dako), PD-L1 (clone E1L3N, Cell Signaling Technology), and KI67 (clone MIB-1, Dako). All the markers were stained in sequence using their respective fluorophores contained in the Opal 7 kit (catalogue #NEL797001KT; Akoya Biosciences, Waltham, MA) and the individual tyramide signal amplification fluorophores in the Opal Polaris 480 (catalog #FP1500001KT) and Opal Polaris 780 (catalog #FP1501001KT, Akoya Biosciences) kits (39). The slides were scanned using the Vectra/Polaris 3.0.3 (Akoya Biosciences) at low magnification, 10x (1.0 μm/pixel), through the full emission spectrum and using positive human reactive tonsil controls (donated from pediatric tonsillectomies) from the run staining to calibrate the spectral image scanner protocol (40). A pathologist selected 5 regions of interest (ROIs) for scanning in high magnification using the Phenochart Software image viewer 1.0.12 (931 × 698 μm at resolution 20x) in order to capture various elements of tissue heterogeneity. Each ROI was analyzed by a pathologist using InForm 2.4.8 image analysis software (Akoya Biosciences). The different ROIs were grouped according to the presence or absence of CK expression in the tumor (groups or nests of malignant T-cells) and stroma (represented by the stroma area between tumor cells) compartments, respectively (40). Marker co-localization was used to identify specific cell phenotypes in the different compartments. Densities of each cell phenotype were quantified, and the final data were expressed as number of cells/mm (40). All the data were consolidated using the R studio 3.5.3 (Phenopter 0.2.2 packet, Akoya Biosciences).

Cytotoxicity assay

Patient and donor T-cell products (except one donor, which was used fresh) were removed from vapor phase liquid nitrogen storage and thawed in warm Hanks' Balanced Salt Solution (HBSS, Cytiva Life Sciences, SH30588.01) supplemented with 10% human AB serum (HuAB, Gemini Bioproducts, 100–512). Thawed cells were resuspended in TexMACS medium (Miltenyi Biotec, 130–097-196) supplemented with 5% HuAB ("Complete TexMACS") containing 50 U/mL benzonase (Sigma-Aldrich, E1014) and placed into T25 flasks. Flasks were rested at 37°C and 5% CO2 overnight. The next day, tumor line flasks were rinsed with plain PBS and trypsinized to detach adherent cells. Cells were collected and washed in Dulbecco's Modified Eagle's Medium (DMEM, ATCC, 30–2002) supplemented with 10% fetal bovine serum (FBS, Avantor Seradigm, 89510–194). Washed tumor lines were resuspended in Complete TexMACS. 1×10^4 cells were plated into each well of a flat-bottomed 96-well plate and incubated for 1 to 4 hours at 37°C to allow tumor cells to adhere during T-cell preparation. Tumor lines used were: UACC257 ($PRAME^{high}$, $COL6A3^{neg}$), Hs695T ($PRAME^{low}$, $COL6A3^{neg}$), SW982 ($PRAME^{low}$, $COL6A3^{low}$), and T98G ($PRAME^{neg}$, $COL6A3^{high}$); all stably expressed NucLight RFP. For 10:1 effector-to-target (E:T) ratio, $1{\times}10^5$ cells T cells and for 5:1 E:T ratio, $5{\times}10^4$ T cells were added

in quadruplicate to appropriate wells in Complete TexMACS medium. Plates containing adhered tumor cell lines and T-cell products were placed into an IncuCyte set to scan for red-fluorescing tumor cells at 2-to-4-hour intervals for 72 hours. Total counts of RFP^+ cells per image were exported, and fold-expansion of RFP^+ cells was calculated by normalizing counts at subsequent timepoints to the earliest clear imaging timepoint (either 0 hours or 4 hours).

Statistical analysis

Descriptive statistics were used to summarize patients' characteristics. Tumor responses were assessed using RECIST1.1. OS was measured from the time of patient consent for the treatment part of the trial until death from any cause or last follow-up. PFS was defined as the time from entry onto the treatment part of the trial until disease progression or death, whichever came first. Survival curves were estimated by using the Kaplan-Meier method, and the median survival was reported with 95% confidence intervals. The log-rank test was used to compare survival between two groups. The data cut-off date for survival analysis was January 21, 2021. Area under the curve (AUC) was calculated for the indicated parameters and time window using the trapezoid rule in GraphPad Prism (patients with missing data were excluded from the analysis). Pearson's correlation coefficient was used in correlation analyses between the two parameters assessed. A paired *t*-test was used for grouped comparison. EC_{50} values were calculated using a nonlinear regression model (4PL). All statistical analyses were conducted using GraphPad Prism except for the survival analyses in Supplemental Figure S4, for which Stata/SE version 17.0 (StataCorp, College Station, Texas) was used. In addition, R was used in the Supplemental Figure S2 heatmaps of the CTCAE v5.0 grading and Supplemental Figure S10E qPCR target expression.

Data Availability

Data are available upon reasonable request. The datasets used and/or analyzed during the current study are available from the corresponding author on reasonable request and approval from study sponsor and institution according to available guidelines at the time of request. Data on TCRβ sequencing are publicly available in Genbank under OQ884263 - OQ884356.

Consent for publication

Patient consent for publication was not required. Patients consented to participate in the study.

RESULTS

Patients

From July 2017 to January 2020, 214 patients were enrolled (Supplemental Figure S1). Ninety-nine (46.3%) patients were HLA-A*02:01-positive, and of those patients, 61 (28.5%) underwent a tumor biopsy. Sixty of 61 biopsies were evaluable for target expression; 54 of these expressed ≥1 target. Forty-three (15.9%) of the 214 patients completed leukapheresis, and manufacturing was initiated for 97 products (2.3 products/patient). Fifty-seven products were successfully released for 36 patients (16.8% of all patients). The remaining products

were not released owing to lack of antigen-specific T-cell precursors in patients' PBMCs (52.5%), failure to meet release requirements (42.5%), or contamination (5.0%). Of the 18 patients who consented to treatment, four did not receive T-cell product due to brain metastases at screening for treatment (n=1), worsening performance status (PS, n=2), or because the T-cell product did not meet infusion criteria (cryostorage bag was found damaged when thawed, n=1, patient ID13). Fifteen patients underwent lymphodepletion, including the 14 who received T-cell products. Table 1 and Supplemental Table S4 summarize the baseline characteristics of the 15 treated patients. The median age was 44 years (range, 20–63), and 13 (86.7%) were female. The median number of prior therapies was 5 (range, 3–12). Patient biomarker expression is listed in Table 1. All patients received bridging therapy (Supplemental Table S5). Supplemental Figure S1B shows the timeline from leukapheresis to T-cell infusion for all 15 patients.

Treatment

The median number of T-cell products administered was two (range, 1–3). Seven (50.0%) patients received one product; three (21.4%) received two products; and four (28.6%) patients received three products, each. The median number of viable cells infused into a patient across all products administered was 1.7×10^{10} cells (range, 0.42 to 3.96×10^{10}), and the median frequency of target-specific $CD3^{+}CD8^{+}$ T cells in the product was 72.0% (Supplemental Table S6), resulting in a median dose of 1.19×10^{10} target-specific T cells (range, 0.1×10^{10} - 3.02×10^{10}). Four patients were treated in Cohort 1 and 10 patients were to be treated in Cohort 2, but two patients did not receive atezolizumab because they did not meet the hematological criteria (Table 1, Supplemental Table S4). Twelve patients received 28 doses of IL2 as per protocol (Supplemental Table S5). One patient (ID14) was taken off study because the T-cell product did not meet infusion criteria as the cryostorage bag was found damaged when thawed.

Safety

Treatment was overall well-tolerated in this heavily pretreated patient population. Treatment-emergent adverse events (TEAEs) are listed in Table 2. The most common adverse events were Grade 1–2 CRS and cytopenias. No ICANS or autoimmune toxicity was encountered. CRS was reported in 10 (71.4%) of 14 patients who received T-cell products (Grade 1, n=6; Grade 2, n=4). All 15 patients developed Grade 4 neutropenia and lymphopenia, which resolved within 1–2 weeks after T-cell infusion, and 8 (53.3%) patients developed Grade 3–4 thrombocytopenia (Supplemental Figure S2). Five (33.3%) patients experienced infectious complications (Grade 3 bacteremia, n=2; port catheter-related infection, n=2; Grade 3 appendicitis, n=1). Other TEAEs included nausea, vomiting, and anorexia. One patient (ID03) developed Grade 3 sinus bradycardia on Day 9 after T-cell therapy; IL2 was discontinued, and the bradycardia resolved by day 15. The patient was a hemochromatosis gene carrier (one copy of the *H63D* mutation). The cardiac work-up was normal. A patient (ID14) with small-cell sarcoma of the mandible experienced Grade 3 QTc interval prolongation (Day 100 after T-cell therapy) associated with hypokalemia. Another patient (ID09) developed Grade 3 orthostatic hypotension on Day 23 and was diagnosed with brain metastases by day 64 after T-cell therapy (Table 2).

Clinical outcomes

Response: Fourteen patients completed treatment and were evaluable for response. No objective responses were noted. At 6 weeks, 12 (85.7%) patients had stable disease (SD) (Table 1). Prolonged disease stabilization was noted in three patients (ID04, 08, 10), lasting for 12.9, 7.3, and 13.7 months, respectively. Patient ID04 received one COL6A3-specific T-cell product and experienced disease stabilization for 12.9 months, with resolution of disease-related pain. Tumor biopsies at 8.0 and 12.13 months after T-cell infusion demonstrated tumor necrosis. Patient ID08, who received three T-cell products (COL6A3, MMP1, and MXRA5) and atezolizumab had SD lasting for 7.3 months. Patient ID10 with peritoneal mesothelioma received one PRAME-specific T-cell product and atezolizumab and had SD lasting for 13.7 months; this patient also received palliative radiotherapy 7 months after T-cell therapy. Patient ID05 with squamous cell carcinoma (SCC) of the anus received two T-cell products (COL6A3 and PRAME) and showed a 26% decrease in tumor measurements (Supplemental Figure S3) at week 6 after T-cell therapy. Response and clinical events are shown in a swimmer plot in Figure 2, and changes in tumor measurement from baseline over time are illustrated in a spider plot in Supplemental Figure S4A.

Survival: Thirteen of 14 treated patients experienced progressive disease (PD). The median PFS was 3.4 months (range,1.8–13.7 months; 95% CI, 2.0–7.4 months) (Table 1, Supplemental Figure S4B). The median OS was 9.4 months (95% CI, 4.7 – 22.2 months) (Supplemental Table S7, Supplemental Figure S4C). No treatment-related deaths were observed. Eleven patients died of PD. Four patients (ID01, 02, 03, 04) had prolonged OS (>20 months). Two patients (ID08, 10) were alive at the time of the analysis.

Immunomonitoring studies and correlation with progression-free survival

Infused T cells were tracked and characterized in patients' blood via flow cytometry-based immunomonitoring. Although target-specific T cells were rarely detected prior to IMA101 T-cell infusion, peak frequencies of up to 78.74% target-specific cells of $CD8^+$ T cells (median 25.58%, range 0.39–78.74%) were observed 1–3 weeks after infusion. Persisting T cells were detected up to 79 weeks (Figure 3A–B). The frequencies observed over time varied among patients, as well as for the products (up to three) infused into the same patient (Supplemental Figure S5A). This variance was not clearly attributed to absolute counts of target-specific cells per microliter of blood (Supplemental Figure S5A) or the number of infused target-specific T cells (Supplemental Figure S5B–C). A correlation trend between the number of infused cells and persistence was observed. This would have reached statistical significance if the outlier in Supplemental Figure S5B (patient ID10) had been disregarded. T-cell kinetics in the blood (AUC of T-cell frequencies over time) demonstrated a trend towards longer PFS in patients with high AUC (Figure 3C). However, due to the small number of patients, statistically significant conclusions could not be drawn.

Phenotypic analysis of target-specific T cells revealed variable expression of CD27, CD28, and CD127 between T-cell products of different patients (Figure 3D). These markers, known to be associated with T-cell survival, increased after infusion. Resting of the products for 44 hours in the absence of cytokines showed no induction of CD27, suggesting a specific induction of these markers in patients post-infusion (Supplemental Figure S5D).

Products showed high frequencies of $CD45RO^+$ cells and low frequencies of $CD45RA^+$ cells, suggesting a predominant effector memory phenotype. CD45RO expression decreased and CD45RA expression increased after infusion, indicating a shift towards terminal differentiation (Figure 3D, Supplemental Figure S7A). Except for TIM-3, which decreased after infusion, no expression of co-inhibitory markers (e.g., PD-1, LAG-3) was observed after infusion (Supplemental Figure S7A).

High levels of the effector molecules CD107a, MIP1β, TNFα, and IFNγ and lower levels of IL2 were found in most products after target restimulation (Supplemental Figure S7B). The frequencies of functional and polyfunctional cells within the $CD8^+$ T-cell fraction decreased after infusion, mostly in line with the declining frequencies of target-specific T cells after the initial peak (Figure 3E–F, Supplemental Figure S9). Exceptions were patients ID04 and ID10, in whom only a fraction of target-specific T cells could exert effector functions. T-cell functionality was similar in all T-cell products manufactured for an individual patient but showed variability across patients. Whereas T-cell functionality showed a steady decline in some patients, functionality was maintained after infusion in others, as shown by the relative expression of effector molecules.

Detection of target-specific T cells in post-treatment tumor tissue

The overall T-cell infiltration in tumor tissue assessed via TCRβ sequencing varied between patients (median, 4.99%; range, 0.1–20.3% of total cells) in the pre-treatment tumor, and no significant change was observed between pre- and post-treatment tumors (Figure 4A, Supplemental Figure S10A). Target-specific T cells were mostly undetectable in pre-treatment tumor tissue (Figure 4B). However, they were detected in post-treatment tumor tissue (median, 0.90%; range, 0–4.17% of total cells), indicating that the target-specific T-cells traffic into the tumor. No significant correlation was observed between overall T-cell infiltration of tumor tissue prior to treatment and infiltration of target-specific T cells after treatment (Supplemental Figure S10B). However, the AUC of target-specific T-cell frequencies in the blood correlated with the frequency of target-specific tumoral T cells, suggesting that high T-cell persistence in the blood may support infiltration of target-specific T cells in the tumor (Supplemental Figure S10C). There was no relevant correlation between the clonal cell number infused and tumoral T-cell infiltration (Supplemental Figure S10D). Notably, target mRNA assessment by qPCR in post-treatment tumor biopsies did not reveal general antigen loss (Supplemental Figure S10E).

Analysis of the spatial distribution of total T cells ($CD3^+$, irrespective of specificity) in the tumor and their phenotypes via multiplex immunofluorescence in two patients with clinical benefit demonstrated fewer $CD3^+$ T cells per mm^2 in patient ID05 compared with patient ID08 both before and after treatment (Figure 4C), which is in line with the results observed by TCRβ sequencing. Although both patients had similar numbers of $CD3^+CD8^+$ T cells per mm^2 prior to treatment, patient ID05 showed an 11-fold decrease in $CD3^+CD8^+$ T cells, even though we observed initial tumor shrinkage in this patient. Patient ID08, who had higher T-cell infiltration, showed prolonged disease stabilization and a nine-fold increase in $CD3^+CD8^+$ T cells. Ten percent of $CD3^+CD8^+$ T cells in the post-treatment tumor expressed the proliferation marker Ki67, which was undetectable before treatment. The ratio between

$CD3^+CD8^+$ T cells and regulatory T cells increased 17-fold from pre- to post-treatment tissue (0.12 and 2.16, respectively). Patients without clinical benefit showed low numbers of infiltrating $CD3^+$ and $CD3^+CD8^+$ T cells (Supplemental Table S8). Given that patients with multiple indications were included in this study, statistically significant differences cannot be reached, and sampling bias due to tumor heterogeneity cannot be excluded.

Detection of T-cell clones with high-avidity TCRs in blood and tumor

IMA101 T-cell products showed varying clonality, and the clonal composition of target-specific T cells was assessed after treatment in blood and tumor (Figure 5A, Supplemental Figure S11). T-cell clones considered to be target-specific were those identified from the pHLA-multimer-sorted population of the respective T-cell products. When adding up frequencies of those target-specific clones for each product or patient, the TCRβ-sequencing revealed results comparable to the frequencies observed by flow-based immunomonitoring, including that pre-treatment target-specific T-cell clones were mostly undetectable (Supplemental Figure S12A). In most cases, only one or a few target-specific T-cell clones contributed to the high frequency in the blood post-treatment, and the most abundant clone in the T-cell product usually remained the most abundant clone post-treatment (Figure 5A, Supplemental Figure S11). However, there were cases where a clone with lower frequency in the T-cell product outgrew the other target-specific clones and became dominant in the blood post-treatment (e.g., COL6A3-C3 in patient ID05).

The ability of selected T-cell products to kill target-positive tumor cell lines was assessed *in vitro*. T cells were able to lyse tumor cell lines expressing the cognate target gene at high levels (UACC257 for PRAME; T98G for COL6A3 target; Figure 5B), with the limitation that COL6A3-specific Product 3 showed only minimal growth inhibition of the target-high cell line T98G. Growth of the tumor cell line Hs695T, which expresses PRAME at low levels, was only marginally inhibited by the PRAME-specific T-cell products. At the same time, TCR-engineered T cells used as controls robustly killed tumor cell lines, even those with low target expression. To understand TCR functional avidity of the target-specific T-cell clones, we identified and characterized TCRs from eleven T-cell products from six patients. The individual TCRs showed a broad range of avidities, with the majority (77.8%, 28/36 characterized TCRs) being of intermediate-low avidity (EC_{50}>10 nM) (Figure 5C). Only five of eleven T-cell products analyzed contained ≥1 high-avidity TCR (EC_{50} ≤10 nM), and only one of those high-avidity clones was infused at a cell number $>10^{10}$ (Supplemental Figure S12B). Seven of eight clones with high avidity showed below average persistence in blood (AUC) and below average frequency in post-treatment tumor tissue (average across all assessed clones; Supplemental Figure S12C–D). No statistically significant association between persistence and avidity was noted.

Infectious complications

Two patients developed Grade 3 bacteremia: patient ID01 (*Staphylococcus simulans*) on Day 38 after T-cell therapy and patient ID10 (*Serratia marcescens*) on Day 41 after T-cell therapy; patient ID10 also experienced Grade 3 cellulitis around the port catheter on Day 17 after T-cell infusion (no organism was identified). Two patients developed Grade 3 device (port catheter)-related infection: patient ID02 (*Streptococcus agalactiae*) on Day 59 after

T-cell therapy and ID07 (*Mycobacterium canariasence*) on Day -3 of lymphodepletion. One patient (ID09) on Day 16 after T-cell therapy developed Grade 3 appendicitis and was treated successfully with IV antibiotics.

Selected patients with clinical benefit

In patient ID04 (SCC of nasopharynx) who received one COL6A3 T-cell product and showed SD for 12.9 months, the high frequency of target-specific T cells in the blood mainly consisted of one clone (Supplemental Figure S12). This clone showed a peak frequency of ~64.9% of T cells and was still at ~14.4% at week 12, which was the last time point assessed by TCRβ-sequencing. Flow-based assessment showed 6.8% of target-specific T cells among $CD3^+CD8^+$ T cells 79 weeks after infusion (Figure 3A–B), which is likely to consist of the one clearly dominant clone. The clone also was detected with ~11.8% of T cells and 1.8% of total cells in the tumor biopsy (Supplemental Figure S12). Overall, patient ID04 showed higher overall tumor infiltration compared to other patients analyzed, which may have promoted the infiltration of the infused target-specific T cells (Figure 4A–B). Assessment of functional avidity of the dominant clone revealed very low avidity (Supplemental Figure S12), which may explain why the tumor growth was stabilized but no tumor shrinkage could be achieved despite the very high abundance of this clone in the blood and tumor.

An example of multi-target activity may be patient ID08 (ovarian cancer), who received three T-cell products against COL6A3, MXRA5, and MMP1 and showed disease stabilization for 7.3 months. At least one clone from every product contributed, with a peak frequency of >5% of T cells, to the overall persistence of up to 60.7% in the peripheral blood and 30.8% of T cells in the tumor biopsy (Supplemental Figure S12). Overall, patient ID08 showed high T-cell infiltration in the tumor and an increase in $CD3^+CD8^+$ T cells that expressed the proliferation marker Ki67, suggesting active infiltration and proliferation of target-specific T cells in the tumor that may have contributed to transient tumor control (Figure 4). The patient showed a high frequency of polyfunctional cells in the T-cell product that maintained their activity post-infusion (Supplemental Figure S10). However, characterization of functional avidity of the highest-frequency COL6A3 clone revealed only low avidity (Supplemental Figure S12).

Patient ID05 (SCC of anus) received two T-cell products (PRAME and COL6A3) and showed a tumor shrinkage of 26% (RECIST1.1) 6 weeks post-infusion. Both T-cell products contained high-avidity clones (Supplemental Figure S12) and showed expression of multiple effector molecules, indicating their functionality (Figure 3E). However, upon infusion all the high-avidity clones showed rather low persistence (peak frequency, <5% of T-cells) in the blood, whereas one COL6A3 clone of low avidity, that was not the highest frequency clone in the T-cell product, gained dominance and contributed most of the target-specific T cells in the blood (peak frequency, 10.2% of T cells) and post-infusion biopsy specimen (2.9% of T cells) (Figure 5A). The outgrowth of this clone suggests that despite its low avidity, this clone may have recognized its target and mediated the tumor shrinkage. At week 8, the frequency of this clone in the blood substantially decreased, accompanied by a pronounced shift of T-cell phenotype towards terminal differentiation and a decrease in expression of effector molecules (Supplemental Figure S10). These observations together

with a low frequency of target-specific T-cells detected in the tumor biopsy may provide a possible explanation for the limited and only short-lived tumor shrinkage followed by disease progression at week 12. The effector-to-target ratio within the tumor may have been too low to achieve a meaningful and durable tumor responses.

DISCUSSION

Clinical trials addressing multiple targets have been conducted previously, for example, in the context of tumor vaccines (46). IMA101 applies the concept to ACT with endogenous T cells (14) and demonstrates the feasibility and tolerability of an actively personalized, multi-target, multi-T-cell product approach for treatment of solid cancers, guided by confirmed target expression in patient-derived biopsies. The combined target positivity rate of 90% among HLA-A*02:01-positive patients demonstrates that this approach can be applied to many patients and can overcome the challenges of having few suitable targets available for ACT and their low prevalence. The capability to initiate manufacture of T-cell products for multiple targets led to the successful generation of ≥1 T-cell product for 36 of the 43 patients (83.7%) who underwent leukapheresis. A limitation of the study was the long manufacturing time of approximately 9 weeks, during which patients received bridging anticancer therapy, resulting in 25 (58.1%) of 43 patients being ineligible for treatment at the time of product release.

The optimal lymphodepleting regimen for T-cell-based therapy in solid tumors has not been established and may differ from the less-intensive regimens applied for approved chimeric antigen receptor (CAR)-T cell therapies in hematological cancers. We previously designed a modified lymphodepleting regimen that was based on the synergistic interactions between FLU and CY, explored in modeled cell line studies (47,48). The dose, timing, and sequence of FLU/CY were different than those used in other protocols and are crucial for synergistic lymphodepletion without excessive normal organ toxicity (47,48). The synergy between FLU and CY may have allowed us to achieve remarkable T-cell expansion and persistence of the infused T cells for a prolonged period of time. T cells were infused 2 days after completion of the 4-day lymphodepleting regimen, thus allowing sufficient time for FLU clearance (32,33).

A low-dose IL2 regimen (1×10^6 IU, s.c. twice daily) was used instead of the high-dose regimen (720,000 IU/kg IV, every 8 hours), which is more widely used with ACT (32,33), to reduce IL2-mediated toxicities while preserving the beneficial effect of IL2 on T-cell persistence (49,50). Known preferential expansion of regulatory T cells by low-dose IL2 (51–53) may be less of a concern in fully lymphodepleted patients. One case of sinus bradycardia on Day 9 after T-cell therapy resulted in discontinuation of IL2. Although it is possible that IL2 contributed to this event, the patient’s bradycardia may also have been, to some extent, associated with them being a carrier of the hereditary hemochromatosis gene (*H63D* mutation).

IMA101 treatment was overall safe and well-tolerated in heavily pretreated patients with relapsed/refractory solid tumors. The safety profile observed with IMA101 compares favorably to what has been reported for CAR-T trials in relapsed or refractory diffuse

large B-cell lymphoma (54), as detailed in Supplemental Table S9. Observed transient cytopenias following lymphodepletion were expected, while a low incidence of serious infections was noted during the neutropenic period. In our study, there was no treatment-related mortality within 100 days of T-cell infusion, and the adverse events, including CRS-like symptoms, were milder and less frequent than those reported in the CAR-T studies that utilized different lymphodepletion regimens (21,22). Furthermore, patients received prophylaxis against bacterial, viral, and fungal infections, keeping the rate of infectious complications low. The lack of ICANS in our study is likely attributable to the absence of active brain metastases. Other contributing factors may include the choice of the targets, the manufacturing process, and more physiological activation of T cells through the natural TCR compared to CAR-T treatment in hematological malignancies (23–25).

It has been demonstrated before that ACT targeting multiple antigens could be a promising approach. Treatment with autologous, non-engineered, multi-target T cells combined with chemotherapy associates with prolonged tumor control in multiple myeloma (55) and pancreatic adenocarcinoma (56); antigen escape was observed in one patient whose T-cell product recognized only one antigen (55). In our trial, we did not observe an association between patient outcomes and the number of products infused or the target(s) addressed. Prolonged disease stabilization, lasting longer than six months, was noted in three patients (ID04, 08, 10), which is considered encouraging for such heavily pretreated patients. Interestingly, two of these three patients (ID08 and 10) received IMA101 in combination with atezolizumab. The latter patient (ID10) had previously experienced disease progression on two investigational checkpoint inhibitors. Although no robust conclusion can be drawn regarding attribution to atezolizumab, IMA101, or their synergy, other investigators have indicated that combining checkpoint blockade and T-cell therapy may result in synergistic antitumor activity (3,20), improved response rates, and persistence of the infused T cells (4,20).

T-cell engraftment and persistence compared favorably to what has been described for similar ACT approaches (57). Interestingly, a high level of T-cell persistence seemed beneficial for prolonged PFS. Multiple factors may have contributed to this robust T-cell persistence, including the modified lymphodepletion and IL2 regimen, the targets themselves, as well as the manufacturing process and thus the phenotype of the infused T cells. T-cell products exhibited a polyfunctional effector memory phenotype with expression of CD45RO, CD127, and CD27. Maintained or even induced expression of CD28, CD27, and CD127 post-infusion with no induction of immune checkpoints post-infusion indicates a long-lived, non-differentiated effector memory phenotype with a maintained capacity to signal through these molecules and only a slow shift towards terminal differentiation and less polyfunctional T cells post-infusion. A comparable phenotype was described in previous studies using a very similar manufacturing process including IL21, where improved T-cell persistence and objective responses were observed (58).

As expected, target-specific T cells were rarely detected prior to infusion, indicating T-cell priming from the naïve repertoire during the manufacturing process (57). IMA101 T cells were detected in post-treatment biopsies of all analyzed patients, suggesting that they can enter the tumor as a prerequisite for antitumor activity. Although T-cell products

were generally able to kill target-positive cell lines, their potency in this respect was heterogeneous and inferior to TCR-engineered T cells. In line with this observation, characterization of individual TCRs in the endogenous T-cell products showed a broad range of avidity, with the majority being intermediate to low (EC_{50} >10 nM), reflecting the range that is expected in the natural immune repertoire directed towards self-epitopes. No general correlation between avidity and persistence was observed, even though the rare high-avidity T-cell clones mostly showed low persistence. This does not suggest a causal relationship, and by the clinical activity and persistence described with high-avidity TCR-engineered T cells supports this lack of causality (58).

Connecting the detailed characterization of the pre- and post-infusion T-cell products with the clinical course of the patients revealed some intriguing observations. Patient ID04 (SCC of nasopharynx) received one COL6A3 T-cell product and showed very high T-cell engraftment and persistence, as well as post-infusion tumor infiltration. Infused and persisting T cells mainly consisted of one dominant T-cell clone with low functional avidity, which may explain why the IMA101 treatment stabilized the patient's disease for 12.9 months but could not achieve an objective response. Another patient (ID05, SCC of anus) showed a 26% decrease in tumor measurements 6 weeks after infusion of two T-cell products (PRAME and COL6A3). Both T-cell products contained high-avidity clones and were multi-functional. However, the high-avidity clones showed low engraftment in the blood, whereas one COL6A3 clone of low avidity gained dominance and contributed to the majority of the post-treatment target-specific T cells in the blood, suggesting that this clone may have recognized its target and mediated the tumor shrinkage. At week 8, the frequency of this clone in the blood significantly decreased, accompanied by a marked shift of T-cell phenotype towards terminal differentiation (re-expression of CD45RA) and a decrease in expression of effector molecules. These findings, combined with a low frequency of tumoral target-specific T cells, may provide an explanation for the disease progression of this patient at week 12, although other causal or contributing intrinsic or acquired resistance mechanisms of the tumor cannot be excluded. Significantly higher T-cell infiltration into the tumor was observed in patient ID08 (ovarian cancer). This patient received three T-cell products, against COL6A3, MXRA5, and MMP1, and showed disease stabilization for 7.3 months. An increase in $CD3^+CD8^+$ T cells expressing the proliferation marker Ki67 suggested active infiltration and proliferation of target-specific T cells in the tumor, which may have contributed to tumor control.

Despite the promising biological data and interesting case studies, no objective responses were observed. The limited data do not allow robust conclusions regarding the clinical activity of IMA101. Possible antitumor activity of the lymphodepleting chemotherapy regimen or of atezolizumab as a single agent could not be distinguished from IMA101 activity. The main barrier to the presented approach reaching clinical efficacy appears to be the limited frequency of highly potent target-specific TCRs in the endogenous T-cell products. This limitation could be overcome by adoptive transfer of autologous TCR-engineered T cells. This approach intends to enhance antitumor activity by using well-characterized, potent, and high-avidity target-specific TCRs. Furthermore, this therapeutic strategy has a shorter manufacturing time and will, thus, accelerate treatment availability

and potentially improve patient outcomes. Respective trials are ongoing (NCT03686124, NCT03441100, NCT03247309).

In conclusion, our study demonstrates that treatment using T cells directed against multiple defined pHLA targets is feasible and, overall, well-tolerated in heavily pretreated patients with advanced, metastatic solid tumors. T-cell persistence, as well as tumor infiltration, was observed. These interesting case studies provided insights into tumor control mechanisms. Our results suggest that high and durable T-cell persistence, a favorable T-cell phenotype, high TCR avidity, or tumor infiltration alone may each be insufficient for efficient antitumor activity. These observations warrant further evaluation of multi-target ACT approaches, preferentially using potent, high-avidity autologous TCR-engineered T cells against defined pHLA targets.

Supplementary Material

Refer to Web version on PubMed Central for supplementary material.

Acknowledgements

This research was funded by Immatics Biotechnologies GmbH, Tuebingen, Germany and supported by the Cancer Prevention Research Institute of Texas (DP150029). Support was also provided in part by the National Institutes of Health/National Cancer Institute under award number P30CA016672. Supported in part by donor funds from Jamie's Hope, Mr. and Mrs. Zane W. Arrott, and Mr. and Mrs. Steven McKenzie for Dr. Tsimberidou's Personalized Medicine Program. The authors would like to thank the patients, their families, and caregivers for participating in the study. They would also like to thank Erik A. Farrar and Mamta Kalra, employees of IMMATICS US Inc, who performed some experiments.

Financial support:

This research was funded by Immatics Biotechnologies GmbH, Tuebingen, Germany and supported by the Cancer Prevention Research Institute of Texas (DP150029). Support was also provided in part by the National Institutes of Health/National Cancer Institute under award number P30CA016672. Supported in part by donor funds from Jamie's Hope, Mr. and Mrs. Zane W. Arrott, and Mr. and Mrs. Steven McKenzie for Dr. Tsimberidou's Personalized Medicine Program.

LIST OF ABBREVIATIONS

ACT	adoptive cell therapy
AUC	area under the curve
CAR	chimeric antigen receptor
CRS	cytokine release syndrome
CTCAE	common terminology criteria of adverse events
CY	cyclophosphamide
ECOG	eastern cooperative oncology group
FLU	fludarabine
HLA	human leukocyte antigen

ICANS	immune effector cell-associated neurotoxicity syndrome
ICS	intracellular cytokine staining
IL	interleukin
IV	intravenous
OS	overall survival
PBMCs	peripheral blood mononuclear cells
PD	progressive disease
PFS	progression-free survival
pHLA	peptide-HLA
PS	performance status
qPCR	quantitative polymerase chain reaction
RACE	rapid amplification of cDNA ends
s.c.	subcutaneous
SCC	squamous cell carcinoma
SD	stable disease
TCR	T-cell receptor
TEAEs	treatment-emergent adverse events

REFERENCES

1. Yee C, Thompson JA, Byrd D, Riddell SR, Roche P, Celis E, et al. Adoptive T cell therapy using antigen-specific CD8+ T cell clones for the treatment of patients with metastatic melanoma: in vivo persistence, migration, and antitumor effect of transferred T cells. Proc Natl Acad Sci U S A 2002;99(25):16168–73 doi 10.1073/pnas.242600099. [PubMed: 12427970]
2. Hunder NN, Wallen H, Cao J, Hendricks DW, Reilly JZ, Rodmyre R, et al. Treatment of metastatic melanoma with autologous CD4+ T cells against NY-ESO-1. N Engl J Med 2008;358(25):2698–703 doi 10.1056/NEJMoa0800251. [PubMed: 18565862]
3. Chapuis AG, Thompson JA, Margolin KA, Rodmyre R, Lai IP, Dowdy K, et al. Transferred melanoma-specific CD8+ T cells persist, mediate tumor regression, and acquire central memory phenotype. Proc Natl Acad Sci U S A 2012;109(12):4592–7 doi 10.1073/pnas.1113748109. [PubMed: 22393002]
4. Chapuis AG, Ragnarsson GB, Nguyen HN, Chaney CN, Pufnock JS, Schmitt TM, et al. Transferred WT1-reactive CD8+ T cells can mediate antileukemic activity and persist in post-transplant patients. Sci Transl Med 2013;5(174):174ra27 doi 10.1126/scitranslmed.3004916.
5. Rosenberg SA. Finding suitable targets is the major obstacle to cancer gene therapy. Cancer Gene Ther 2014;21(2):45–7 doi cgt20143 [pii];10.1038/cgt.2014.3 [doi]. [PubMed: 24535159]
6. Yee C, Lizee G, Schueneman AJ. Endogenous T-Cell Therapy: Clinical Experience. Cancer J 2015;21(6):492–500 doi 10.1097/PPO.0000000000000158. [PubMed: 26588682]

7. Linette GP, Stadtmauer EA, Maus MV, Rapoport AP, Levine BL, Emery L, et al. Cardiovascular toxicity and titin cross-reactivity of affinity-enhanced T cells in myeloma and melanoma. Blood 2013;122(6):863–71 doi 10.1182/blood-2013-03-490565. [PubMed: 23770775]
8. Robbins PF, Morgan RA, Feldman SA, Yang JC, Sherry RM, Dudley ME, et al. Tumor regression in patients with metastatic synovial cell sarcoma and melanoma using genetically engineered lymphocytes reactive with NY-ESO-1. J Clin Oncol 2011;29(7):917–24 doi 10.1200/JCO.2010.32.2537. [PubMed: 21282551]
9. Robbins PF, Kassim SH, Tran TL, Crystal JS, Morgan RA, Feldman SA, et al. A pilot trial using lymphocytes genetically engineered with an NY-ESO-1-reactive T-cell receptor: long-term follow-up and correlates with response. Clin Cancer Res 2015;21(5):1019–27 doi 10.1158/1078-0432.CCR-14-2708. [PubMed: 25538264]
10. Rapoport AP, Stadtmauer EA, Binder-Scholl GK, Goloubeva O, Vogl DT, Lacey SF, et al. NY-ESO-1-specific TCR-engineered T cells mediate sustained antigen-specific antitumor effects in myeloma. Nat Med 2015;21(8):914–21 doi 10.1038/nm.3910. [PubMed: 26193344]
11. Johnson LA, Morgan RA, Dudley ME, Cassard L, Yang JC, Hughes MS, et al. Gene therapy with human and mouse T-cell receptors mediates cancer regression and targets normal tissues expressing cognate antigen. Blood 2009;114(3):535–46 doi 10.1182/blood-2009-03-211714. [PubMed: 19451549]
12. Khong HT, Restifo NP. Natural selection of tumor variants in the generation of “tumor escape” phenotypes. Nat Immunol 2002;3(11):999–1005 doi 10.1038/ni1102-999. [PubMed: 12407407]
13. Gerlinger M, Rowan AJ, Horswell S, Math M, Larkin J, Endesfelder D, et al. Intratumor heterogeneity and branched evolution revealed by multiregion sequencing. N Engl J Med 2012;366(10):883–92 doi 10.1056/NEJMoa1113205. [PubMed: 22397650]
14. Britten CM, Singh-Jasuja H, Flamion B, Hoos A, Huber C, Kallen KJ, et al. The regulatory landscape for actively personalized cancer immunotherapies. Nat Biotechnol 2013;31(10):880–2 doi 10.1038/nbt.2708. [PubMed: 24104749]
15. Chapuis AG, Lee SM, Thompson JA, Roberts IM, Margolin KA, Bhatia S, et al. Combined IL-21-primed polyclonal CTL plus CTLA4 blockade controls refractory metastatic melanoma in a patient. J Exp Med 2016;213(7):1133–9 doi 10.1084/jem.20152021. [PubMed: 27242164]
16. Yee C, Thompson JA, Byrd D, Riddell SR, Roche P, Celis E, et al. Adoptive T cell therapy using antigen-specific CD8+ T cell clones for the treatment of patients with metastatic melanoma: in vivo persistence, migration, and antitumor effect of transferred T cells. Proc Natl Acad Sci U S A 2002;99(25):16168–73. [PubMed: 12427970]
17. Chapuis AG, Ragnarsson GB, Nguyen HN, Chaney CN, Pufnock JS, Schmitt TM, et al. Transferred WT1-reactive CD8+ T cells can mediate antileukemic activity and persist in post-transplant patients. Sci Transl Med 2013;5(174):174ra27 doi 5/174/174ra27 [pii];10.1126/scitranslmed.3004916 [doi].
18. Klebanoff CA, Khong HT, Antony PA, Palmer DC, Restifo NP. Sinks, suppressors and antigen presenters: how lymphodepletion enhances T cell-mediated tumor immunotherapy. Trends Immunol 2005;26(2):111–7 doi 10.1016/j.it.2004.12.003. [PubMed: 15668127]
19. Dudley ME, Yang JC, Sherry R, Hughes MS, Royal R, Kammula U, et al. Adoptive cell therapy for patients with metastatic melanoma: evaluation of intensive myeloablative chemoradiation preparative regimens. J Clin Oncol 2008;26(32):5233–9 doi 10.1200/JCO.2008.16.5449. [PubMed: 18809613]
20. Chapuis AG, Roberts IM, Thompson JA, Margolin KA, Bhatia S, Lee SM, et al. T-Cell Therapy Using Interleukin-21-Primed Cytotoxic T-Cell Lymphocytes Combined With Cytotoxic T-Cell Lymphocyte Antigen-4 Blockade Results in Long-Term Cell Persistence and Durable Tumor Regression. J Clin Oncol 2016;34(31):3787–95 doi 10.1200/JCO.2015.65.5142. [PubMed: 27269940]
21. Houot R, Schultz LM, Marabelle A, Kohrt H. T-cell-based Immunotherapy: Adoptive Cell Transfer and Checkpoint Inhibition. Cancer Immunol Res 2015;3(10):1115–22 doi 10.1158/2326-6066.CIR-15-0190. [PubMed: 26438444]
22. Yoon DH, Osborn MJ, Tolar J, Kim CJ. Incorporation of Immune Checkpoint Blockade into Chimeric Antigen Receptor T Cells (CAR-Ts): Combination or Built-In CAR-T. Int J Mol Sci 2018;19(2) doi 10.3390/ijms19020340.

23. Chong EA, Melenhorst JJ, Lacey SF, Ambrose DE, Gonzalez V, Levine BL, et al. PD-1 blockade modulates chimeric antigen receptor (CAR)-modified T cells: refueling the CAR. Blood 2017;129(8):1039–41 doi 10.1182/blood-2016-09-738245. [PubMed: 28031179]
24. Heczey A, Louis CU, Savoldo B, Dakhova O, Durett A, Grilley B, et al. CAR T Cells Administered in Combination with Lymphodepletion and PD-1 Inhibition to Patients with Neuroblastoma. Mol Ther 2017;25(9):2214–24 doi 10.1016/j.ymthe.2017.05.012. [PubMed: 28602436]
25. Zacharakis N, Chinnasamy H, Black M, Xu H, Lu YC, Zheng Z, et al. Immune recognition of somatic mutations leading to complete durable regression in metastatic breast cancer. Nat Med 2018;24(6):724–30 doi 10.1038/s41591-018-0040-8. [PubMed: 29867227]
26. Fritsche J, Rakitsch B, Hoffgaard F, Romer M, Schuster H, Kowalewski DJ, et al. Translating Immunopeptidomics to Immunotherapy-Decision-Making for Patient and Personalized Target Selection. Proteomics 2018;18(12):e1700284 doi 10.1002/pmic.201700284. [PubMed: 29505699]
27. Neelapu SS, Tummala S, Kebriaei P, Wierda W, Gutierrez C, Locke FL, et al. Chimeric antigen receptor T-cell therapy - assessment and management of toxicities. Nat Rev Clin Oncol 2018;15(1):47–62 doi 10.1038/nrclinonc.2017.148. [PubMed: 28925994]
28. Gutierrez C, McEvoy C, Mead E, Stephens RS, Munshi L, Detsky ME, et al. Management of the Critically Ill Adult Chimeric Antigen Receptor-T Cell Therapy Patient: A Critical Care Perspective. Crit Care Med 2018;46(9):1402–10 doi 10.1097/CCM.0000000000003258. [PubMed: 29939878]
29. Weinschenk T, Gouttefangeas C, Schirle M, Obermayr F, Walter S, Schoor O, et al. Integrated functional genomics approach for the design of patient-individual antitumor vaccines. Cancer Res 2002;62(20):5818–27. [PubMed: 12384544]
30. Tsimberidou AM, Stewart C, Reinhardt C, Ma H, Walter S, Weinschenk T, et al. Phase I adoptive cellular therapy trial with ex-vivo stimulated autologous CD8+ T-cells against multiple targets (ACTolog IMA101) in patients with relapsed and/or refractory solid cancers. Journal of Clinical Oncology 2018;36(5_suppl):TPS77-TPS doi 10.1200/JCO.2018.36.5_suppl.TPS77.
31. Tsimberidou A, Ma H, Stewart C, Schoor O, Maurer D, Mendrzyk R, et al. Phase I adoptive cellular therapy trial with ex-vivo stimulated autologous CD8+ T-cells against multiple targets (ACTolog® IMA101) in patients with relapsed and/or refractory solid cancers. ESMO 2018 Congress Annals of Oncology 2018;29 (suppl_8).
32. Long-Boyle JR, Green KG, Brunstein CG, Cao Q, Rogosheske J, Weisdorf DJ, et al. High fludarabine exposure and relationship with treatment-related mortality after nonmyeloablative hematopoietic cell transplantation. Bone Marrow Transplant 2011;46(1):20–6 doi 10.1038/bmt.2010.53. [PubMed: 20383215]
33. Sanghavi K, Wiseman A, Kirstein MN, Cao Q, Brundage R, Jensen K, et al. Personalized fludarabine dosing to reduce nonrelapse mortality in hematopoietic stem-cell transplant recipients receiving reduced intensity conditioning. Transl Res 2016;175:103–15 e4 doi 10.1016/j.trsl.2016.03.017. [PubMed: 27094990]
34. Lee DW, Santomasso BD, Locke FL, Ghobadi A, Turtle CJ, Brudno JN, et al. ASTCT Consensus Grading for Cytokine Release Syndrome and Neurologic Toxicity Associated with Immune Effector Cells. Biol Blood Marrow Transplant 2019;25(4):625–38 doi 10.1016/j.bbmt.2018.12.758. [PubMed: 30592986]
35. Carlson CS, Emerson RO, Sherwood AM, Desmarais C, Chung MW, Parsons JM, et al. Using synthetic templates to design an unbiased multiplex PCR assay. Nat Commun 2013;4:2680 doi 10.1038/ncomms3680. [PubMed: 24157944]
36. Robins H, Desmarais C, Matthis J, Livingston R, Andriesen J, Reijonen H, et al. Ultra-sensitive detection of rare T cell clones. J Immunol Methods 2012;375(1–2):14–9 doi 10.1016/j.jim.2011.09.001. [PubMed: 21945395]
37. Andersen RS, Kvistborg P, Frosig TM, Pedersen NW, Lyngaa R, Bakker AH, et al. Parallel detection of antigen-specific T cell responses by combinatorial encoding of MHC multimers. Nat Protoc 2012;7(5):891–902 doi 10.1038/nprot.2012.037. [PubMed: 22498709]
38. Hadrup SR, Bakker AH, Shu CJ, Andersen RS, van Veluw J, Hombrink P, et al. Parallel detection of antigen-specific T-cell responses by multidimensional encoding of MHC multimers. Nat Methods 2009;6(7):520–6 doi 10.1038/nmeth.1345. [PubMed: 19543285]

39. Parra ER, Zhai J, Tamegnon A, Zhou N, Pandurengan RK, Barreto C, et al. Identification of distinct immune landscapes using an automated nine-color multiplex immunofluorescence staining panel and image analysis in paraffin tumor tissues. Sci Rep 2021;11(1):4530 doi 10.1038/s41598-021-83858-x. [PubMed: 33633208]
40. Parra ER, Jiang M, Solis L, Mino B, Laberiano C, Hernandez S, et al. Procedural Requirements and Recommendations for Multiplex Immunofluorescence Tyramide Signal Amplification Assays to Support Translational Oncology Studies. Cancers (Basel) 2020;12(2) doi 10.3390/cancers12020255.
41. Garboczi DN, Hung DT, Wiley DC. HLA-A2-peptide complexes: refolding and crystallization of molecules expressed in Escherichia coli and complexed with single antigenic peptides. Proc Natl Acad Sci U S A 1992;89(8):3429–33. [PubMed: 1565634]
42. Robins HS, Campregher PV, Srivastava SK, Wacher A, Turtle CJ, Kahsai O, et al. Comprehensive assessment of T-cell receptor beta-chain diversity in alphabeta T cells. Blood 2009;114(19):4099–107 doi 10.1182/blood-2009-04-217604. [PubMed: 19706884]
43. Kobayashi E, Mizukoshi E, Kishi H, Ozawa T, Hamana H, Nagai T, et al. A new cloning and expression system yields and validates TCRs from blood lymphocytes of patients with cancer within 10 days. Nat Med 2013;19(11):1542–6 doi nm.3358 [pii];10.1038/nm.3358 [doi]. [PubMed: 24121927]
44. Rosa MD. Four T7 RNA polymerase promoters contain an identical 23 bp sequence. Cell 1979;16(4):815–25. [PubMed: 455451]
45. Kozak M An analysis of 5'-noncoding sequences from 699 vertebrate messenger RNAs. Nucleic Acids Res 1987;15(20):8125–48 doi 10.1093/nar/15.20.8125. [PubMed: 3313277]
46. Hilf N, Kuttruff-Coqui S, Frenzel K, Bukur V, Stevanovic S, Gouttefangeas C, et al. Actively personalized vaccination trial for newly diagnosed glioblastoma. Nature 2019;565(7738):240–5 doi 10.1038/s41586-018-0810-y. [PubMed: 30568303]
47. Yamauchi T, Nowak BJ, Keating MJ, Plunkett W. DNA repair initiated in chronic lymphocytic leukemia lymphocytes by 4-hydroperoxycyclophosphamide is inhibited by fludarabine and clofarabine. Clin Cancer Res 2001;7(11):3580–9. [PubMed: 11705880]
48. Valdez BC, Andersson BS. Interstrand crosslink inducing agents in pretransplant conditioning therapy for hematologic malignancies. Environ Mol Mutagen 2010;51(6):659–68 doi 10.1002/em.20603. [PubMed: 20577993]
49. Atkins MB, Kunkel L, Sznol M, Rosenberg SA. High-dose recombinant interleukin-2 therapy in patients with metastatic melanoma: long-term survival update. Cancer J Sci Am 2000;6 Suppl 1:S11–4. [PubMed: 10685652]
50. Rosenberg SA. Interleukin-2 and the development of immunotherapy for the treatment of patients with cancer. Cancer J Sci Am 2000;6 Suppl 1:S2–7. [PubMed: 10685650]
51. Locke FL, Neelapu SS, Bartlett NL, Siddiqi T, Chavez JC, Hosing CM, et al. Phase 1 Results of ZUMA-1: A Multicenter Study of KTE-C19 Anti-CD19 CAR T Cell Therapy in Refractory Aggressive Lymphoma. Mol Ther 2017;25(1):285–95 doi 10.1016/j.ymthe.2016.10.020. [PubMed: 28129122]
52. Neelapu SS, Locke FL, Bartlett NL, Lekakis LJ, Miklos DB, Jacobson CA, et al. Axicabtagene Ciloleucel CAR T-Cell Therapy in Refractory Large B-Cell Lymphoma. N Engl J Med 2017;377(26):2531–44 doi 10.1056/NEJMoa1707447. [PubMed: 29226797]
53. Schuster SJ, Bishop MR, Tam CS, Waller EK, Borchmann P, McGuirk JP, et al. Tisagenlecleucel in Adult Relapsed or Refractory Diffuse Large B-Cell Lymphoma. N Engl J Med 2019;380(1):45–56 doi 10.1056/NEJMoa1804980. [PubMed: 30501490]
54. Tsimberidou AM, Van Morris K, Vo HH, Eck S, Lin YF, Rivas JM, et al. T-cell receptor-based therapy: an innovative therapeutic approach for solid tumors. J Hematol Oncol 2021;14(1):102 doi 10.1186/s13045-021-01115-0. [PubMed: 34193217]
55. Lulla PD, Tzannou I, Vasileiou S, Carrum G, Ramos CA, Kamble R, et al. The safety and clinical effects of administering a multiantigen-targeted T cell therapy to patients with multiple myeloma. Sci Transl Med 2020;12(554) doi 10.1126/scitranslmed.aaz3339.
56. Smaglo BG, Musher BL, Vasileiou S, Kuvalekar M, Watanabe A, Robertson C, et al. A phase I trial targeting advanced or metastatic pancreatic cancer using a combination of standard

chemotherapy and adoptively transferred nonengineered, multiantigen specific T cells in the first-line setting (TACTOPS). J Clin Oncol 2020;suppl; abstract 4622:4622.

57. Chapuis AG, Desmarais C, Emerson R, Schmitt TM, Shibuya K, Lai I, et al. Tracking the Fate and Origin of Clinically Relevant Adoptively Transferred CD8(+) T Cells In Vivo. Sci Immunol 2017;2(8) doi 10.1126/sciimmunol.aal2568.
58. D'Angelo SP, Melchiori L, Merchant MS, Bernstein D, Glod J, Kaplan R, et al. Antitumor Activity Associated with Prolonged Persistence of Adoptively Transferred NY-ESO-1 (c259)T Cells in Synovial Sarcoma. Cancer Discov 2018;8(8):944–57 doi 10.1158/2159-8290.CD-17-1417. [PubMed: 29891538]
59. Wadelin F, Fulton J, McEwan PA, Spriggs KA, Emsley J, Heery DM. Leucine-rich repeat protein PRAME: expression, potential functions and clinical implications for leukaemia. Mol Cancer 2010;9:226 doi 10.1186/1476-4598-9-226. [PubMed: 20799951]
60. Epping MT, Hart AA, Glas AM, Krijgsman O, Bernards R. PRAME expression and clinical outcome of breast cancer. Br J Cancer 2008;99(3):398–403 doi 10.1038/sj.bjc.6604494. [PubMed: 18648365]
61. Ikeda H, Lethe B, Lehmann F, Van BN, Baurain JF, De SC, et al. Characterization of an antigen that is recognized on a melanoma showing partial HLA loss by CTL expressing an NK inhibitory receptor. Immunity 1997;6(2):199–208 doi S1074–7613(00)80426–4 [pii]. [PubMed: 9047241]
62. Hawthorn L, Lan L, Mojica W. Evidence for field effect cancerization in colorectal cancer. Genomics 2014;103(2–3):211–21 doi 10.1016/j.ygeno.2013.11.003. [PubMed: 24316131]
63. Yang S, Shin J, Park KH, Jeung HC, Rha SY, Noh SH, et al. Molecular basis of the differences between normal and tumor tissues of gastric cancer. Biochim Biophys Acta 2007;1772(9):1033–40. [PubMed: 17601708]
64. Karousou E, D'Angelo ML, Kouvidi K, Vigetti D, Viola M, Nikitovic D, et al. Collagen VI and hyaluronan: the common role in breast cancer. Biomed Res Int 2014;2014:606458 doi 10.1155/2014/606458. [PubMed: 25126569]
65. Daudi S, Eng KH, Mhawech-Fauceglia P, Morrison C, Miliotto A, Beck A, et al. Expression and immune responses to MAGE antigens predict survival in epithelial ovarian cancer. PLoS One 2014;9(8):e104099 doi 10.1371/journal.pone.0104099. [PubMed: 25101620]
66. Zamuner FT, Karia BT, de Oliveira CZ, Santos CR, Carvalho AL, Vettore AL. A Comprehensive Expression Analysis of Cancer Testis Antigens in Head and Neck Squamous Cell Carcinoma Revels MAGEA3/6 as a Marker for Recurrence. Mol Cancer Ther 2015;14(3):828–34 doi 1535–7163.MCT-14–0796 [pii];10.1158/1535-7163.MCT-14-0796 [doi]. [PubMed: 25564441]
67. Toh Y, Yamana H, Shichijo S, Fujita H, Tou U, Sakaguchi M, et al. Expression of MAGE-1 gene by esophageal carcinomas. Jpn J Cancer Res 1995;86(8):714–7 doi 091050509591202F [pii]. [PubMed: 7559092]
68. Yamada R, Takahashi A, Torigoe T, Morita R, Tamura Y, Tsukahara T, et al. Preferential expression of cancer/testis genes in cancer stem-like cells: proposal of a novel sub-category, cancer/testis/stem gene. Tissue Antigens 2013;81(6):428–34 doi 10.1111/tan.12113. [PubMed: 23574628]
69. Shafer JA, Cruz CR, Leen AM, Ku S, Lu A, Rousseau A, et al. Antigen-specific cytotoxic T lymphocytes can target chemoresistant side-population tumor cells in Hodgkin lymphoma. Leuk Lymphoma 2010;51(5):870–80 doi 10.3109/10428191003713968 [doi]. [PubMed: 20367572]
70. Lifantseva N, Koltsova A, Krylova T, Yakovleva T, Poljanskaya G, Gordeeva O. Expression patterns of cancer-testis antigens in human embryonic stem cells and their cell derivatives indicate lineage tracks. Stem Cells Int 2011;2011:795239 doi 10.4061/2011/795239 [doi]. [PubMed: 21785609]
71. He Y, Chen X, Liu H, Xiao H, Kwapong WR, Mei J. Matrix-remodeling associated 5 as a novel tissue biomarker predicts poor prognosis in non-small cell lung cancers. Cancer Biomark 2015;15(5):645–51 doi CBM504 [pii];10.3233/CBM-150504 [doi]. [PubMed: 26406953]
72. Buckanovich RJ, Sasaroli D, O'Brien-Jenkins A, Botbyl J, Hammond R, Katsaros D, et al. Tumor vascular proteins as biomarkers in ovarian cancer. J Clin Oncol 2007;25(7):852–61 doi 25/7/852 [pii];10.1200/JCO.2006.08.8583 [doi]. [PubMed: 17327606]

73. Zou TT, Selaru FM, Xu Y, Shustova V, Yin J, Mori Y, et al. Application of cDNA microarrays to generate a molecular taxonomy capable of distinguishing between colon cancer and normal colon. Oncogene 2002;21(31):4855–62. [PubMed: 12101425]

74. Esfandiary A, Ghafouri-Fard S. New York esophageal squamous cell carcinoma-1 and cancer immunotherapy. Immunotherapy 2015;7(4):411–39 doi 10.2217/imt.15.3. [PubMed: 25917631]

75. Merdad A, Karim S, Schulten HJ, Dallol A, Buhmeida A, Al-Thubaity F, et al. Expression of matrix metalloproteinases (MMPs) in primary human breast cancer: MMP-9 as a potential biomarker for cancer invasion and metastasis. Anticancer Res 2014;34(3):1355–66 doi 34/3/1355 [pii]. [PubMed: 24596383]

76. Cai QW, Li J, Li XQ, Wang JQ, Huang Y. Expression of STAT3, MMP-1 and TIMP-1 in gastric cancer and correlation with pathological features. Mol Med Rep 2012;5(6):1438–42 doi 10.3892/mmr.2012.849. [PubMed: 22469989]

77. Altadill A, Rodriguez M, Gonzalez LO, Junquera S, Corte MD, Gonzalez-Dieguez ML, et al. Liver expression of matrix metalloproteases and their inhibitors in hepatocellular carcinoma. Dig Liver Dis 2009;41(10):740–8 doi 10.1016/j.dld.2009.01.016. [PubMed: 19372066]

Synopsis:

Feasibility and safety of a personalized adoptive cell therapy (ACT) against multiple peptide-HLA cancer targets is demonstrated. Results warrant further investigation regarding the use of multi-targeted ACT approaches with high-avidity TCR products in patients with advanced metastatic cancer.

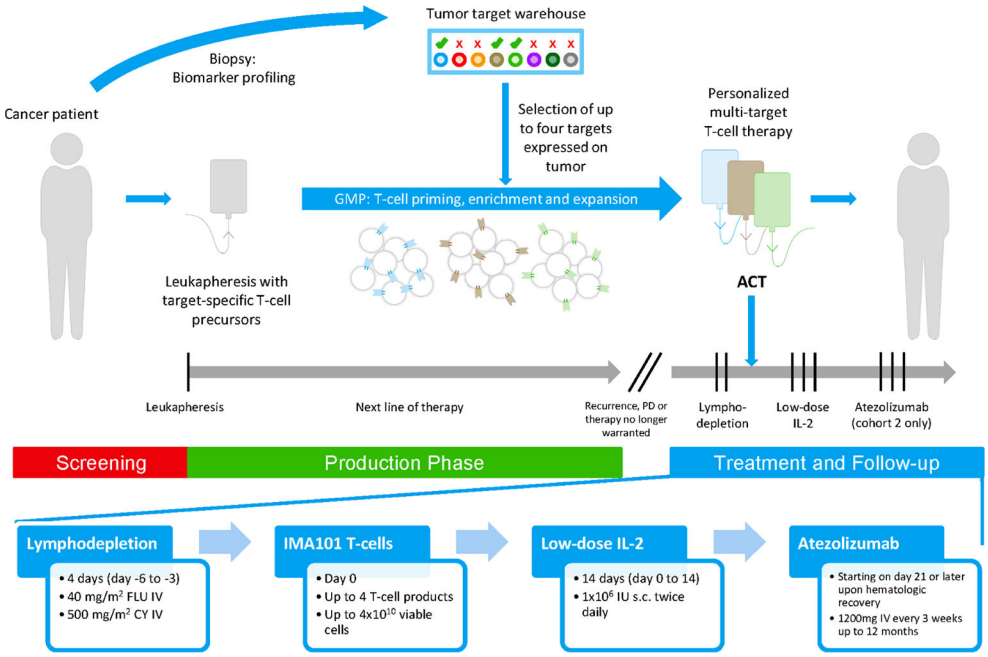

Figure 1. Study schema: IMA101 personalized multi-targeted T-cell therapy.

Patients were screened for tumor targets, and T-cell products were generated. Patients were treated with lymphodepletion, IMA101 infusion, and IL2 with/without atezolizumab (anti-PD-L1), as indicated.

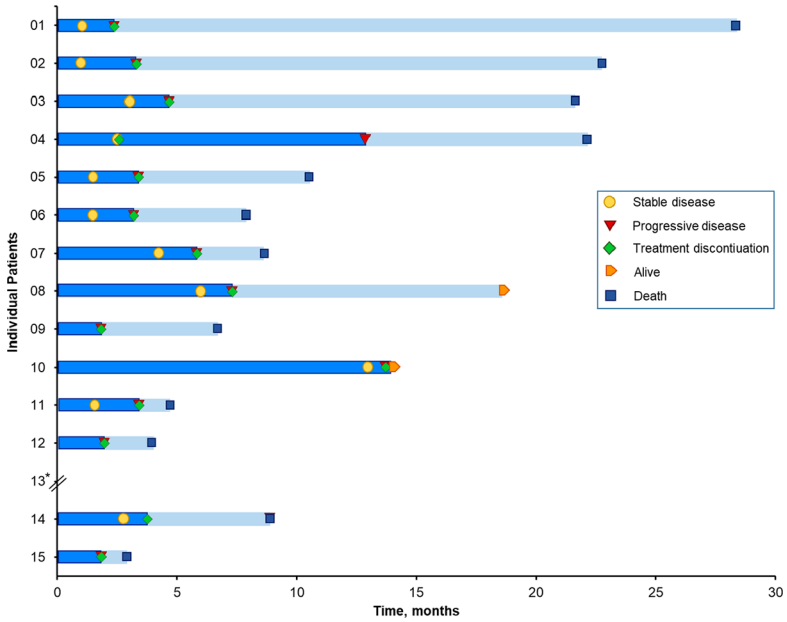

Figure 2. Clinical events in patients who underwent treatment.

Swimmer plot of clinical responses in relationship to duration of treatment and time of treatment discontinuation. Day 0 (infusion of the IMA101 T-cell product) was chosen as baseline (time 0). Symbols along and at the end of each bar represent relevant clinical events. *Patient ID13 was non-evaluable owing to not receiving the T-cell product.

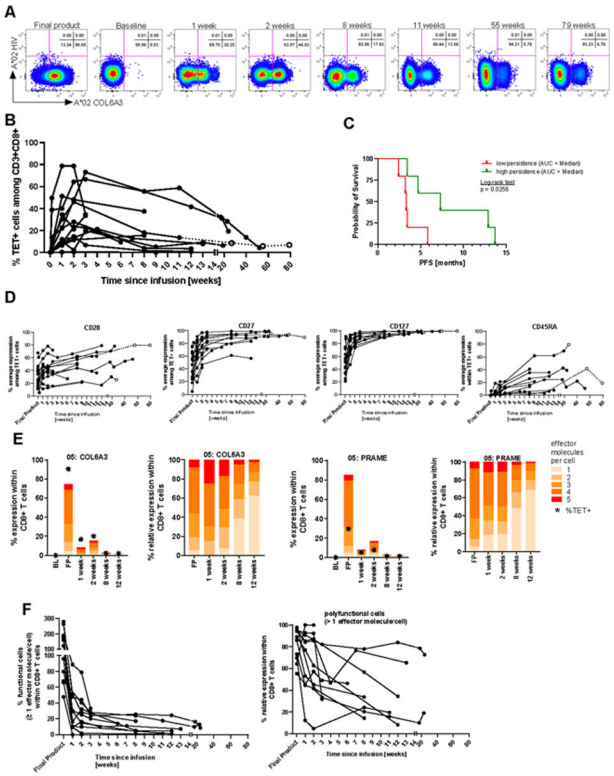

Figure 3. Target-specific T cells show very high frequencies in the blood after infusion and exhibit a favorable T-cell phenotype.

(A) Representative pHLA multimer staining for target-specific T cells in the T-cell products and PBMCs of patient 04 prior to and after infusion. (B) Persistence of target-specific T cells in PBMCs after infusion as assessed by flow cytometry. Frequencies of target-specific T cells (TET^+) among $CD3^+CD8^+$ T cells (sum of specificities) are shown for each patient (n=14, 29 independent experiments were performed). Last data points for each patient indicate either the timepoint of progression or the last sampling timepoint before progression. Data points after progression (follow-up samples) are indicated as open circles. (C) PFS of patients with high (> median, n=5) vs. low (< median, n=5) T-cell persistence (AUC [baseline to week 8] of the T-cell frequencies [$\%TET^+$ of $CD3^+CD8^+$]) in the blood after infusion. (D) Expression of phenotypic markers on pre- and post-infusion target-specific T cells. Average expression is shown for patients who received more than one T-cell product (n=14, 29 independent experiments were performed). Last data points for each patient indicate either the timepoint of progression or the last sampling timepoint before progression. Data points after progression (follow-up samples) are indicated as open circles. (E) Expression of effector molecules in pre- and post-infusion $CD8^+$ T cells after *ex vivo* target restimulation (n=12, 9 independent experiments were performed). Frequency of cells that expressed between 1 and 5 effector molecules are shown within $CD8^+$ T cells (left) and relative to the frequency of cells that express any effector molecule (right). (F) Frequency of functional T cells (≥1 effector molecule) within pre- and post-infusion $CD8^+$ T cells (left. Sum frequencies of functional cells after re-stimulation with the individual targets are shown for patients that received more than one T-cell product. Frequency of polyfunctional T cells (>1 effector molecule) within $CD8^+$ cells that expressed any effector

molecule (right). Average is shown for patients who received more than one T-cell product (n=12, 9 independent experiments were performed. BL=baseline, FP=final T-cell product, p=*p*-value.

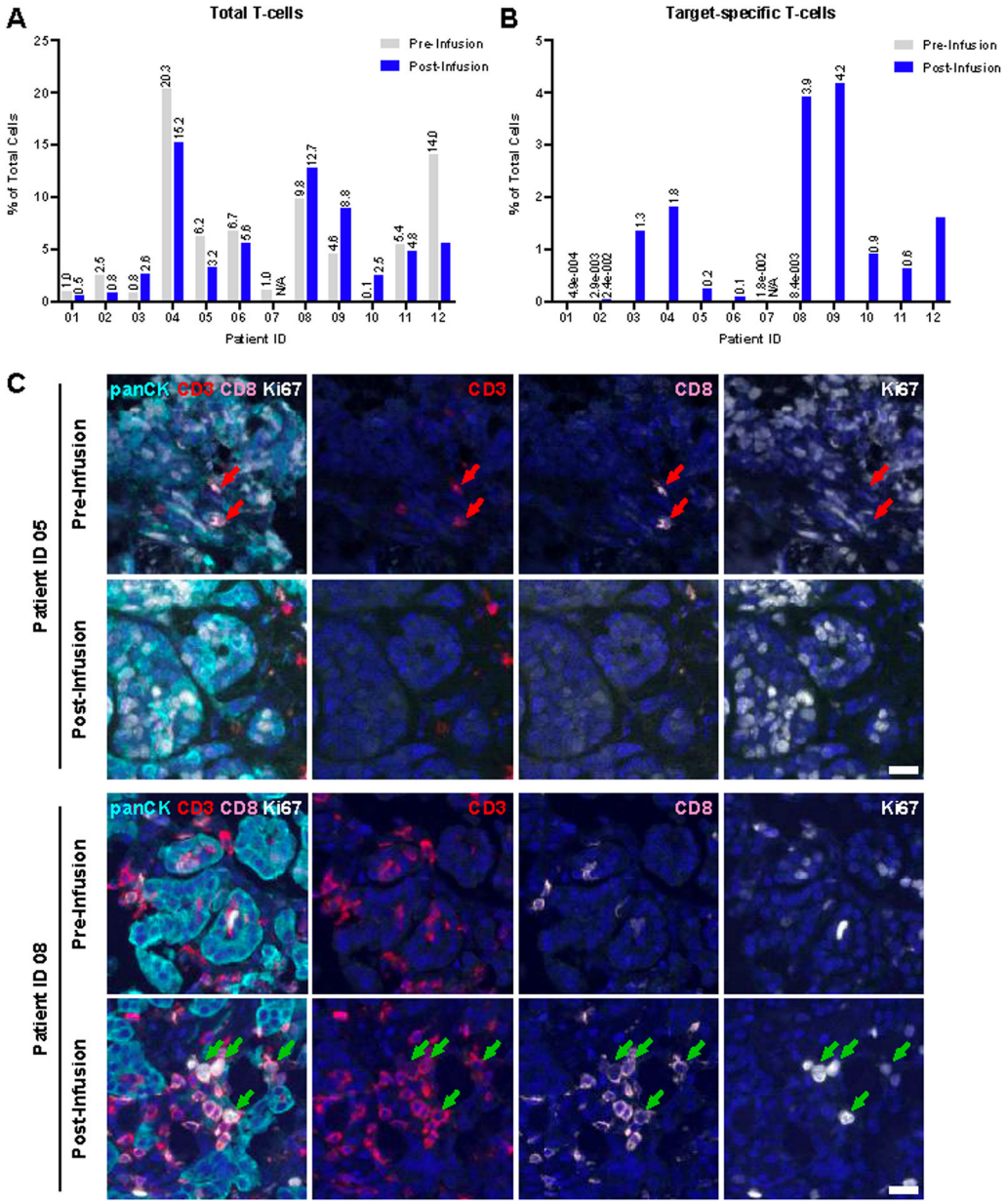

Figure 4. Target-specific T cells can be detected in the tumor after infusion.

(A) Tumor infiltration by T cells as assessed by TCRβ-sequencing. Frequencies of T cells among total cells in tumor biopsy prior to and after infusion (median 6.0 weeks post-infusion) are shown per patient pooled from 5 independent sequencing experiments. (B) Tumor infiltration (median 6.0 weeks post-infusion) by target-specific T cells as assessed by TCRβ-sequencing. Frequencies of target-specific T-cell clones (identified by TCRβ-sequencing from T-cell product sorted with target-specific multimers) among total cells in tumor biopsy prior to and after infusion are shown per patient pooled from 5 independent sequencing experiments. (C) Representative multiplex immunofluorescence images from formalin-fixed, paraffin-embedded core needle biopsies of patient ID05 and patient ID08 before and ≈6 weeks after treatment. Green arrows indicate proliferating, cytotoxic T cells

infiltrating the tumor area after treatment. Red arrows indicate very low levels of cytotoxic T cells before treatment that are almost absent after treatment. $CD3^+$ (red) = T-lymphocyte; $CD3^+CD8^+$ (pink) = cytotoxic T-cell; DAPI (blue) = cell nuclei; Ki67 (white) = proliferating cell; panCK (turquoise) = epithelial (tumor) cells. Scale bar represents 20 μm.

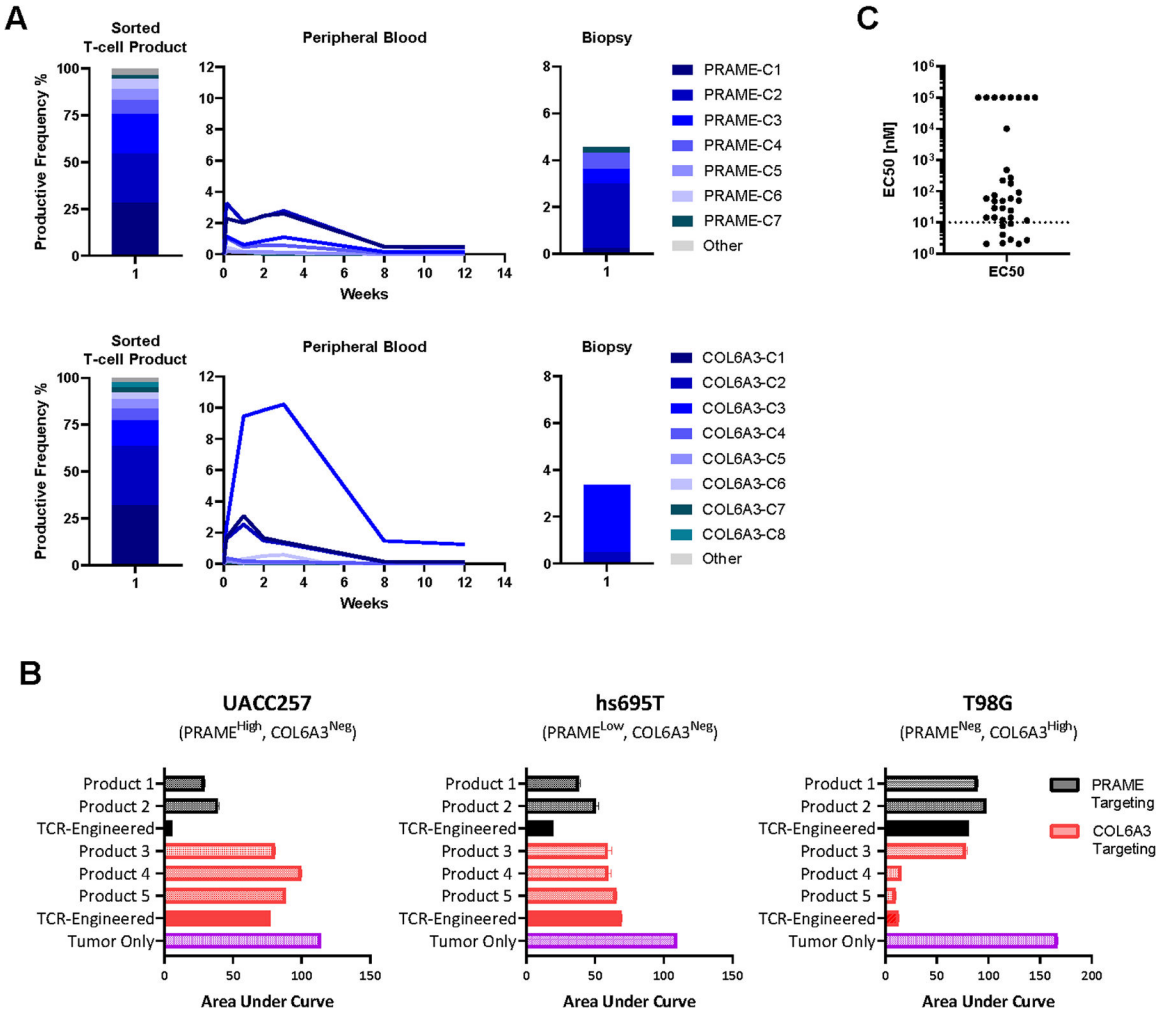

Figure 5. Some IMA101 products contain T-cell clones with high-avidity TCRs that can be found in the blood and tumor.

(A) Target-specific T-cell clones as identified by TCRβ-sequencing from T-cell products sorted with target-specific multimers (left) and tracking of those clones by TCRβ-sequencing in the blood (middle) and tumor biopsy (right) prior to and after infusion. Target-specific T-cell clones were not detectable in tumor biopsies prior to infusion. Representative results are shown for patient ID05. (B) Available IMA101 products with confirmed TCR expression from patients were co-cultured in quadruplicates with tumor cell lines at E:T ratios of 10:1 and 5:1. Tumor cell growth and killing was followed in a Sartorius IncuCyte. Tumor lines were all HLA-A*02:01^{+} and varied in target expression: UACC257 (PRAME^{high}, COL6A3^{neg}; E:T 10:1), hs695T (PRAME^{low}, COL6A3^{neg}; E:T 10:1), and T98G (PRAME^{neg}, COL6A3^{high}; E:T 5:1). The plots show the normalized integrated area under the curve of the fold tumor growth from the earliest clear scan timepoint up through 72 hours of co-culture. TCR-engineered T-cell products were used as reference and positive controls. Error bars represent standard error of mean. (C) Functional avidity of individual TCRs isolated from T-cell products after re-expression in TCRαβ-KO (CD8^{+}) Jurkat cells, which expressed an NFAT-luciferase reporter. EC_{50} values of luciferase activation were determined from co-culture experiments using peptide-loaded T2 target cells. Low-avidity

TCRs of EC_{50} values above the applied peptide loading range (10 pM – 10 μM) were indicated as $EC_{50} = 10^5$ nM. The experiment was performed once in triplicate.

Table 1.

Baseline patient characteristics

Pt. ID	Age, yrs	Sex	Tumor Dx	Date Dx to Rx ICD, yrs	No. of prior systemic Rx	Positive biomarkers	T-cell products received: viable/ specific cells x10^{10}	Total dose, viable/ specific cells x10^{10}	Atezolizumab	RECIST1.1 responseat 6 wks	PFS*, months
01	56	F	Adenocarcinoma of breast	18	10	COL6A3, MXRA5	MXRA5: 0.42/ 0.10	0.42	No	SD	2.4
02	28	F	Synovial sarcoma	10	5	PRAME, COL6A3,MXRA5, NY-ESO-1	PRAME: 1.16/ 0.84MXRA5: 1.02/ 0.42NY-ESO-1: 1.37/ 0.59	3.54	No	SD	3.3
03	36	M	Myxoid liposarcoma	6	12	PRAME, COL6A3, NY-ESO-1	PRAME: 1.16/ 0.76COL6A3: 1.16/ 1.09NY-ESO-1: 1.16/ 1.07	3.48	No	SD	4.7
04	37	M	SCC of nasopharynx	12	5	COL6A3, MMP1	COL6A3: 1.69/ 1.47	1.68	No	SD	12.9
05	58	F	SCC of the anus	4	7	PRAME, COL6A3	PRAME: 0.97/ 0.49COL6A3: 0.76/ 0.26	1.72	Yes	SD	3.4
06	31	F	Infiltrating duct carcinoma of breast	3	7	COL6A3, PRAME, MMP1	COL6A3: 1.61/ 1.27PRAME:0.33/ 0.03	1.92	Yes	SD	3.2
07	49	F	Synovial sarcoma	3	5	PRAME, COL6A3, MXRA5	PRAME: 1.74/ 1.58COL6A3:0.91/ 0.63MXRA5: 1.32/ 0.82	3.96	No	SD	5.8
08	24	F	Ovarian cancer	1	4	COL6A3, MMP1, MXRA5	COL6A3: 1.16/ 0.97MMP1: 1.41/ 0.85MXRA5: 1.16/ 1.00	3.73	Yes	SD	7.3
09	56	F	Invasive duct breast cancer	3	3	COL6A3, NY-ESO-1	COL6A3: 1.04/ 0.89NY-ESO-1: 1.74/ 1.61	2.78	No	PD	1.8
10	63	F	Mesothelioma of peritoneum	6	7	PRAME	PRAME:0.68/ 0.55	0.68	Yes	SD	13.7
11	32	F	Infiltrating ductal carcinoma of breast	4	8	COL6A3	COL6A3: 1.39/ 1.09	1.39	Yes	SD	3.4
12	57	F	Adenocarcinoma of transverse colon	1	5	COL6A3	COL6A3: 0.72/ 0.40	0.72	Yes	PD	2.0
13‡	44	F	Squamous cell cancer of anus	4	3	COL6A3	N/A	N/A	N/A	N/A	N/A
14§	20	F	Small cell sarcoma	5	7	COL6A3	COL6A3: 0.58/ 0.44	0.58	Yes	SD	3.7

Pt. ID	Age, yrs	Sex	Tumor Dx	Date Dx to Rx ICD, yrs	No. of prior sys-temic Rx	Positive bio-markers	T-cell products received: viable/ specific cells x10^{10}	Total dose, viable/ specific cells x10^{10}	Atezo-lizumab	RECIST1.1 responseat 6 wks	PFS*, months
			of mandible								
15	56	F	Adeno-carcinoma of colon	2	4	COL6A3, MMP1	COL6A3: 0.77/ 0.46	0.77	Yes	PD	1.8

Dx, diagnosis; ICD, informed consent document; N/A, not applicable; PFS, progression-free survival; Rx, therapy; SCC, squamous cell carcinoma; SD, stable disease

*Progression-free survival was measured in months from date of entry on the treatment part of the study to date of disease progression or treatment discontinuation

‡Patient 13 received lymphodepletion but did not receive the T-cell product because it was damaged

§Patient 14 withdrew consent after 3.7 months of treatment.

Table 2.

Treatment-emergent adverse events (*N*=15) *

Adverse events	All grades		Grade 1		Grade 2		Grade 3		Grade 4	
	No.	%	No.	%	No.	%	No.	%	No.	%
Cytokine release syndrome **	10	66.7	6	40.0	4	26.7				
Leukopenia	15	100.0							15	100.0
Neutropenia	15	100.0					1	6.7	14	93.37
Lymphopenia	15	100.0							15	100
Thrombocytopenia	14	93.3	4	26.7	2	13.3	4	26.7	4	26.7
Anemia	15	100.0			3	20.0	12	80.0		
Febrile neutropenia	5	33.3	1	6.7	3	20.0	1	6.7		
Chills	4	26.7	3	20.0	1	6.7				
Fever without neutropenia	2	13.3	2	13.3						
Device-related infection	2	13.3					2	13.3		
Bacteremia	2	13.3					2	13.3		
Cellulitis	1	6.7					1	6.7		
Appendicitis	1	6.7					1	6.7		
Nausea	11	73.3	6	40.0	5	33.3				
Vomiting	9	60.0	7	46.7	2	13.3				
Anorexia	5	33.3	4	26.7	1	6.7				
Constipation	7	46.7	5	33.3	2	13.3				
Abdominal pain	3	20.0			2	13.3	1	6.7		
Mucositis	1	6.7					1	6.7		
Dysphagia	1	6.7					1	6.7		
Sinus tachycardia	2	13.3	2	13.3						
Sinus bradycardia	1	6.7					1	6.7		
QT prolongation	1	6.7					1	6.7		
Hypotension	4	26.7	2	13.3	1	6.7	1	6.7		
Orthostatic hypotension	1	6.7					1	6.7		
Hypokalemia	2	13.3	1	6.7			1	6.7		
Fatigue	6	40.0	4	26.7	2	13.3				
Dizziness	5	33.3	4	26.7	1	6.7				
Headache	5	33.3	4	26.7	1	6.7				

* 14 patients received T-cell products and were assessed for CRS; 1 patient with damaged T-cell product storage bag received the lymphodepletion regimen but not the T-cell product.

** Patients are counted only once per adverse event and severity classification (the most severe adverse event is shown).